



## THREE-DIMENSIONAL REACHABLE SET FOR THE DUBINS CAR: FOUNDATION OF ANALYTICAL DESCRIPTION

VALERII PATSKO\*, ANDREY FEDOTOV

Krasovskii Institute of Mathematics and Mechanics, Ekaterinburg, Russia

Dedicated to the memory of Professor Rafail Fedorovich Gabasov

**Abstract.** The Dubins car is a model of motion, in which the scalar control  $u$  determines the instantaneous angular speed of rotation. The paper considers the symmetric variant of the constraints  $u \in [u_1, u_2]$ , where  $u_1 = -u_2$  and  $u_2 = 1$ . We study the three-dimensional reachable set at a given instant  $t_f > 0$ . An analytical description of two-dimensional sections of the set w.r.t. the angular coordinate  $\varphi$  is given. The boundary of each  $\varphi$ -section is formed with the help of a certain set of curves obtained using the Pontryagin maximum principle. This set includes circular arcs and circular involutes. The symmetry property of each  $\varphi$ -section w.r.t. a certain straight line is established. Classification of possible types of the  $\varphi$ -sections is proposed. The greatest difficulty is presented by analysis of the case with non-simply connected  $\varphi$ -sections. The range of values  $\varphi$  and  $t_f$ , at which the  $\varphi$ -sections are non-simply connected, is indicated.

**Keywords.** Dubins car; Extremal piecewise constant control; Pontryagin maximum principle; Sections of reachable set along the angle coordinate; Three-dimensional reachable set.

### 1. INTRODUCTION

The mathematical “Dubins car” is a model of controllable motion, in which two phase variables  $x, y$  are the coordinates of a point geometric position in the plane and the third variable  $\varphi$  is the angle formed by the velocity vector w.r.t. the positive direction of the axis  $x$ . The value of the linear velocity is considered to be constant and equal to 1. The scalar control  $u$  has the sense of the angular speed of rotation (or, equivalently, the instantaneous radius of turn) and is restricted by the constraint  $u \in [-1, 1]$ .

The name of the model is related to work [1], in which L. Dubins established the properties of curves of the minimal length (with a radius of curvature bounded from below) that connect two points in the plane with the specified exit and entry directions. It corresponds to the time-optimal problem for an object moving at the constant speed and rotation radius restricted from

\*Corresponding author.

E-mail address: [patsko@imm.uran.ru](mailto:patsko@imm.uran.ru) (V. Patsko), [andreyfedotov@mail.ru](mailto:andreyfedotov@mail.ru) (A. Fedotov).

Received November 21, 2021; Accepted September 17, 2022.

below. The results obtained by L. Dubins have been reproven and supplemented with the help of the Pontryagin maximum principle in [2, 3].

Speaking about the previous history of the similar problems, we should note article [4] by A.A. Markov, in which he considered four mathematical problems associated with the design of railways. In 1951, R. Isaacs, while working for the Rand Corporation, submitted his first report [5] on the theory of differential games, in which he posed and outlined the solution to the “homicidal chauffeur” problem. It was R. Isaacs who first began to call the described controllable object with the word “car”.

This model is often referred to as the “simplified unicycle”. It is used when considering aircraft motions in the horizontal plane with the constant speed and small bank angles (see, e.g., [6, Chapter 4, Section 8.4], [7]). Such model is also applied to a simplified description of motion of the controllable wheeled “bogies” [8] and autonomous underwater vehicles [9]. The list of meaningful problems in the plane, the mathematical description of which (after some transformations) is reduced to the Dubins model, is available in book [10].

The literature devoted to solving specific control problems using the Dubins car is huge. The most popular are various variants of the time-optimal problem [11, 12, 13, 14, 15, 16] that includes problems with the phase constraints. The time-optimal problems with the requirement of passing through the given points are considered in works [17, 18, 19, 20]. Synthesis of the time-optimal control for the Dubins car under the standard three-dimensional termination condition is presented in paper [7]. The problems of possibility of elongation curves solving the time-optimal problem with the three-dimensional termination condition for a certain period of time are considered in [21]. In some works (e.g., [22, 23, 24]), solutions of the pursuit problems close to game problems are investigated where the pursuer has the dynamics of the Dubins car. Some papers study connection between the standard time-optimal problem of object transferring to a given set in the space of geometric coordinates with the solution of the “homicidal chauffeur” differential game [25, 26, 27].

Work [28] also deserves attention, in which the Dubins car found an unexpected use for soft manipulators.

The constraint on the control does not necessarily have the form  $u \in [-1, 1]$ . A more general variant can be written as  $u \in [u_1, u_2]$ . For the case of  $u_1 < 0$ ,  $u_2 > 0$ , synthesis of the time-optimal control is built in work [29]. Other models of motion are also studied; their description clearly comes from the Dubins car but is more complex [10, Chapter 13], [30, 31, 32, 33]. At the same time, the structure of the optimal controls often inherits the optimal structure of the similar problem with the dynamics of the Dubins car (see, e.g., work [34]).

The reachable set *at an instant*  $t_f$  under the given initial phase state at the instant  $t_0$  is a set of all phase states, into each of which it is possible to transfer the system with the help of some permissible open-loop control exactly at the instant  $t_f$ . The reachable set at the instant  $t_f$  differs from the reachable set *up to the instant*. The latter consists of phase states, into each of which it is possible to transfer the system at some instant from the interval  $[t_0, t_f]$ .

For the numerical construction of the three-dimensional reachable sets, the grid methods (developed in the framework of the differential games theory and Hamilton-Jacobi-Bellman partial differential equations) can be used. Examples of such constructions are given in works [35, 36, 37, 38].

This paper examines the reachable set at an instant  $t_f$ . Let us denote it as  $G(t_f)$ . For the constraint  $u \in [-1, 1]$ , an analytical description of boundary of the two-dimensional sections  $G_\varphi(t_f)$  of the set  $G(t_f)$  by the angular coordinate  $\varphi$  is given. In general, such  $\varphi$ -sections are non-convex and can be non-simply connected. Their structure depends on the instant  $t_f$  and the value  $\varphi$ . Description of the two-dimensional reachable set at an instant in geometric coordinates  $x, y$  (i.e., the projection of the three-dimensional set  $G(t_f)$  into the plane  $x, y$ ) was obtained in work [39].

The results presented in the paper are based on the statements from paper [40] where (with the help of the Pontryagin maximum principle [41, 42]) the statements about 6 types of piecewise constant open-loop control have been proven. One can limit by only these control types when constructing the boundary of the set  $G(t_f)$ . The selected types basically coincide with the variants obtained by L. Dubins in work [1].

Using these 6 types of the open-loop control, we analyze (with a fixed  $t_f$ ) the ends of the corresponding motions that implement the specified value  $\varphi$ . Thus, in the  $\varphi$ -section of the set  $G(t_f)$ , a number of curves are selected and the boundary of the  $\varphi$ -section is constructed with the help of them. For  $\varphi \geq 0$ , we consider 5 different cases of the boundary formation of the  $\varphi$ -section. An analysis of some of these cases is very laborious.

The paper is organized as follows. In Section 2, the problem statement is given. In Section 3, information is given on 6 types of the extreme motions used to construct the boundary of the reachable set  $G(t_f)$ . For  $\varphi \geq 0$ , formulas for curves in the  $\varphi$ -sections generated by extreme motions are derived. An auxiliary coordinate system is considered, which is more convenient than the original one when analyzing the properties of curves in the  $\varphi$ -sections. Some curves are described, from the parts of which the boundary of the  $\varphi$ -sections is constructed. The properties of these curves are analyzed. In particular, it is established that two curves represent parts of the involutes of the circle. Section 4 is devoted to statements about the extreme motions leading to the interior of the set  $G(t_f)$ . Auxiliary statements based on the Jordan curve theorem are given in Section 5. In Section 6, classification of the  $\varphi$ -sections is given depending on the values  $t_f$  and  $\varphi$ . All possible variants are divided into five cases. In Sections 7–10, the detailed analysis of each of these cases is given. Of particular interest is Case 2, for which the  $\varphi$ -sections are not simply connected. Section 12 describes the symmetry property that allows one to find the  $\varphi$ -sections for  $\varphi < 0$  relying on the constructed  $\varphi$ -sections for  $\varphi \geq 0$ .

## 2. PROBLEM STATEMENT

Consider the controllable system

$$\dot{x} = \cos \varphi, \quad \dot{y} = \sin \varphi, \quad \dot{\varphi} = u; \quad u \in [-1, 1]. \quad (2.1)$$

Here,  $x$  and  $y$  are the coordinates of the geometric position in the plane,  $u$  is the scalar control. Let us agree that the positive value of the angle  $\varphi$  is counted from the positive direction of the axis  $x$  counterclockwise (Fig. 1). The phase vector  $(x, y, \varphi)^T$  of system (2.1) will be denoted as  $z$ .

As the initial state at the instant  $t_0 = 0$ , we set  $x_0 = y_0 = \varphi_0 = 0$ . The value of the angle  $\varphi$  at the instant  $t$  is calculated in the form of the integral

$$\int_0^t u(\tau) d\tau$$

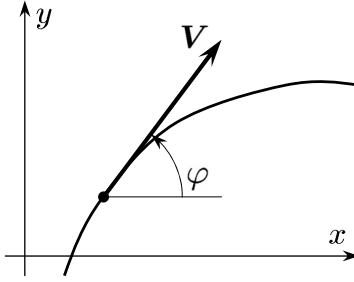


FIGURE 1. The coordinate system,  $\mathbf{V} = (\dot{x}, \dot{y})^\top$

of the open-loop control implemented on the interval  $[0, t]$ . Thus,  $\varphi \in (-\infty, +\infty)$ . As admissible open-loop controls, we take measurable functions of time that satisfy the constraint onto the control  $u$ .

The reachable set  $G(t_f)$  is defined as the set of all those phase states of system (2.1) that can be obtained *at the instant*  $t_f$  using all the admissible measurable open-loop controls on the interval  $[0, t_f]$ . The choice of measurable controls as admissible is due to the desire to talk about the closedness of the reachable set  $G(t_f)$  within the framework of the problem statement.

By the symbol  $G_\varphi(t_f)$ , we denote the  $\varphi$ -section of the set  $G(t_f)$ :

$$G_\varphi(t_f) = \{(x, y)^\top : (x, y, \varphi)^\top \in G(t_f)\}.$$

The purpose of this work is to obtain an analytical description of the  $\varphi$ -sections.

The symbol  $\partial$  will mean the boundary of the set, the symbol “int” is its interior. Note that if some point  $P$  belongs to  $\partial G_\varphi(t_f)$ , then the point  $(P, \varphi)^\top$  belongs to  $\partial G(t_f)$ . Generally speaking, the reverse is not true.

### 3. PROPERTIES OF CURVES GENERATED BY EXTREME MOTIONS

**3.1. Types of extreme motions.** We apply the Pontryagin maximum principle (PMP) to the open-loop controls transferring system (2.1) onto the boundary of the reachable set. Under this, we establish that for any point on the boundary there is some *piecewise constant* control leading to this point. The corresponding calculations are given in [40, 43]. It is shown that any point on the boundary of a three-dimensional set  $G(t_f)$  can be reached using an open-loop control that takes values in the three-element set  $\{-1, 0, 1\}$  and has no more than two switch instants. We identified 6 types of controls, by which one can limit to study the boundary.

Let us list these 6 types. The switch instants are denoted by  $t_1$  and  $t_2$ . We suppose that  $t_0 = 0$ ,  $t_f > 0$  and  $t_0 \leq t_1 \leq t_2 \leq t_f$ .

Any control of the type U1 takes the value  $u = 1$  at some first time interval  $[0, t_1)$ , the value  $u = 0$  is applied on some second interval  $[t_1, t_2)$ , and the value  $u = 1$  is used on the third interval  $[t_2, t_f]$ . If one or two of the specified intervals are missing, then the resulting control is also assigned to the U1 type. The types U2 – U6 are defined similarly. Noting the control values on each of three intervals, we shall write the corresponding table in the form

$$\begin{aligned} \text{U1: } & 1, 0, 1; & \text{U2: } & -1, 0, 1; & \text{U3: } & 1, 0, -1; \\ \text{U4: } & -1, 0, -1; & \text{U5: } & 1, -1, 1; & \text{U6: } & -1, 1, -1. \end{aligned} \tag{3.1}$$

These types of controls coincide with those ones that were identified by L. Dubins in work [1] for solving the time-optimal problem. In relation to the controls of the types U5 and U6, additional conditions have been noted in the L. Dubins' work that are specific namely for the time-optimal problem. In the problem of constructing the boundary of the reachable set  $G(t_f)$ , the additional requirement for controls of the types U5 and U6 has the following form [40, p. 323]:

$$t_2 - t_1 \geq (t_1 - t_0) + (t_f - t_2). \quad (3.2)$$

In [40], it is shown that when inequality (3.2) is violated, the open-loop control of the types U5 or U6 leads to the interior of the reachable set  $G(t_f)$ .

Since the controls U1 – U6 satisfy the PMP, we call them and corresponding motions extreme. For the controls U5 and U6, in the sequel, we shall assume that inequality (3.2) is fulfilled.

For each type of control, degeneration (reducing to zero) is possible of one or two intervals of control constancy. Formally, we shall refer such controls to more than one type of controls U1 – U6 specified in (3.1).

The set of possible values  $\varphi$  of system (2.1) at the instant  $t_f > 0$  is defined by the constraint  $u \in [-1, 1]$  and represents the segment  $[-t_f, t_f]$ . The extreme values  $\varphi = \mp t_f$  are provided on the controls  $u(t) \equiv \mp 1$ . We get the single-point  $\varphi$ -sections with the coordinates  $x(t_f) = \sin t_f$ ,  $y(t_f) = \mp(1 - \cos t_f)$ .

For  $\varphi > 0$ , only four (namely, U1, U2, U3, and U6) from six types of control (specified in (3.1)) can lead to the boundary  $\partial G_\varphi(t_f)$  of the corresponding  $\varphi$ -section. Indeed, any control of the type U4 gives the value  $\varphi \leq 0$  at the instant  $t_f$ . For any control of the type U5 with  $\varphi > 0$ , condition (3.2) is violated. We emphasize that for any control of type U6 for  $\varphi \geq 0$ , the condition (3.2) is satisfied.

Let  $\varphi = 0$  at the instant  $t_f$ . Then the control of the type U4 is identically equal to zero and can also be assigned to the type U1. Now we take an arbitrary control of the type U5 with the switch instants  $t_1$  and  $t_2$ . We have  $t_0 \leq t_1 \leq t_2 \leq t_f$  and  $t_2 - t_1 = (t_f - t_2) + (t_1 - t_0)$ . Consider the control of the type U6 with the switches at the instants  $t_1^* = t_f - t_2$  and  $t_2^* = t_1^* + (t_2 - t_1)$ . Integrating system (2.1), it is easy to verify that the designed control of the type U6 leads to the same point  $(x(t_f), y(t_f))^T$  as the initial control of the type U5. Therefore, for  $\varphi = 0$ , the controls of the type U5 generate the same set of points  $(x, y)^T$  at the instant  $t_f$  as the controls of the type U6.

Thus, the following lemma is valid.

**Lemma 3.1.** *For  $\varphi \in [0, t_f)$ , to construct the boundary of the  $\varphi$ -sections of the reachable set  $G(t_f)$ , one can restrict themselves to four types of controls U1, U2, U3, and U6.*

Further, when studying the  $\varphi$ -sections, detailed calculations are made under the assumption  $0 \leq \varphi < t_f$ . The constructed  $\varphi$ -sections (taking into account the symmetry of system (2.1)) determine the  $\varphi$ -sections for the condition  $-t_f < \varphi < 0$  using some linear transformation.

**3.2. Formulas in the original coordinates for curves in  $\varphi$ -sections.** Fixing a certain value of  $\varphi$  at the instant  $t_f > 0$ , we get a connection between the switch instants  $t_1$  and  $t_2$  which provides this  $\varphi$ . Thus, for each control type providing the selected  $\varphi$ , we get corresponding one-parameter curve in the plane  $x, y$ .

We assume that  $\varphi \geq 0$ . In accordance with Lemma 3.1, we use controls of the types U1, U2, U3, and U6 to construct the boundary of the  $\varphi$ -sections.

Introduce the notation  $\theta = (t_f - \varphi)/2$ . Obviously, for  $\varphi \in [0, t_f)$ , the inequalities  $\theta > 0$  and  $\theta + \varphi > 0$  are fulfilled.

We give formulas describing the geometric positions in the plane  $x, y$  by virtue of controls of the types U1, U2, U3, and U6 for the selected values  $t_f$  and  $\varphi$ . The corresponding one-dimensional parameters  $s_1, s_2, s_3$ , and  $s_6$  are determined using the formulas

$$s_1 = 2t_1 - \varphi, \quad s_2 = -t_1, \quad s_3 = t_1 - \varphi, \quad s_6 = 2t_1 - \theta. \quad (3.3)$$

We shall take the ranges of acceptable values of these parameters (marking the begin and end values) in the form

$$\begin{aligned} s_1 \in [s_1^b, s_1^e] &= [-\varphi, \varphi], & s_2 \in [s_2^b, s_2^e] &= [-\theta, 0], \\ s_3 \in [s_3^b, s_3^e] &= [0, \theta], & s_6 \in [s_6^b, s_6^e] &= [-\theta, \theta]. \end{aligned} \quad (3.4)$$

Integrating system (2.1) for four types of the controls under consideration, we get four curves in the plane  $x, y$ :

$$\begin{pmatrix} x_{U1}(s_1) \\ y_{U1}(s_1) \end{pmatrix} = \begin{pmatrix} \sin \varphi \\ 1 - \cos \varphi \end{pmatrix} + (t_f - \varphi) \begin{pmatrix} \cos \left( \frac{s_1 + \varphi}{2} \right) \\ \sin \left( \frac{s_1 + \varphi}{2} \right) \end{pmatrix}, \quad (3.5)$$

$$\begin{pmatrix} x_{U2}(s_2) \\ y_{U2}(s_2) \end{pmatrix} = \begin{pmatrix} \sin \varphi \\ 1 - \cos \varphi \end{pmatrix} + 2 \left( (\theta + s_2) \begin{pmatrix} \cos s_2 \\ \sin s_2 \end{pmatrix} - \begin{pmatrix} \sin s_2 \\ 1 - \cos s_2 \end{pmatrix} \right), \quad (3.6)$$

$$\begin{pmatrix} x_{U3}(s_3) \\ y_{U3}(s_3) \end{pmatrix} = - \begin{pmatrix} \sin \varphi \\ 1 - \cos \varphi \end{pmatrix} + 2 \left( (\theta - s_3) \begin{pmatrix} \cos(s_3 + \varphi) \\ \sin(s_3 + \varphi) \end{pmatrix} + \begin{pmatrix} \sin(s_3 + \varphi) \\ 1 - \cos(s_3 + \varphi) \end{pmatrix} \right), \quad (3.7)$$

$$\begin{pmatrix} x_{U6}(s_6) \\ y_{U6}(s_6) \end{pmatrix} = - \begin{pmatrix} \sin \varphi \\ 1 - \cos \varphi \end{pmatrix} + 4 \sin \left( \frac{t_f + \varphi}{4} \right) \begin{pmatrix} \cos \left( \frac{\varphi - s_6}{2} \right) \\ \sin \left( \frac{\varphi - s_6}{2} \right) \end{pmatrix}. \quad (3.8)$$

In work [44], other (but equivalent) formulas for the parametric representation of the indicated curves in the original coordinate system  $x, y$  were obtained. They were used there for the analytical description of the  $\varphi$ -sections in the assumption  $t_f \leq 2\pi$ . The relations (3.5)–(3.8) are more compact and more effective for the analysis of the  $\varphi$ -sections under any value  $t_f > 0$ .

**3.3. Auxiliary coordinate system.** We shall use an auxiliary orthogonal coordinate system as in work [44]. It is convenient for revealing the symmetry properties of the  $\varphi$ -sections boundary. We define the auxiliary system  $X, Y$  through the original system  $x, y$  as follows:

$$\begin{pmatrix} X \\ Y \end{pmatrix} = \begin{pmatrix} \cos(\varphi/2) & \sin(\varphi/2) \\ -\sin(\varphi/2) & \cos(\varphi/2) \end{pmatrix} \left( \begin{pmatrix} x \\ y \end{pmatrix} - \begin{pmatrix} \sin \varphi \\ 1 - \cos \varphi \end{pmatrix} \right). \quad (3.9)$$

For a fixed  $\varphi$ , this linear transformation consists of a rotation and a shift. It is one-to-one and preserves the distance between points.

The axis  $X$  of the auxiliary system passes through the origin of the initial system (point  $o$ ) and is rotated by an angle  $\varphi/2$  counterclockwise relative to the axis  $x$  (Fig. 2). The reference point of the auxiliary system (point  $O$ ) coincides with the center of the circumference containing arc (3.5). The axis  $X$  divides this arc in half.

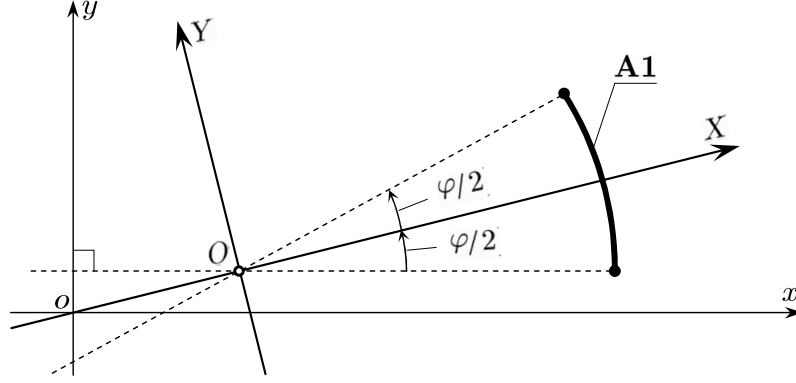


FIGURE 2. Auxiliary coordinate system  $X, Y$

We denote by  $A1, A2, A3,$  and  $A6$  curves (3.5), (3.6), (3.7), and (3.8), which are generated by the controls  $U1, U2, U3,$  and  $U6$  in the auxiliary system. Their analytical representation has the form

$$A1(s_1) = \begin{pmatrix} X_{U1}(s_1) \\ Y_{U1}(s_1) \end{pmatrix} = (t_f - \varphi) \begin{pmatrix} \cos\left(\frac{s_1}{2}\right) \\ \sin\left(\frac{s_1}{2}\right) \end{pmatrix} = 2\theta \begin{pmatrix} \cos\left(\frac{s_1}{2}\right) \\ \sin\left(\frac{s_1}{2}\right) \end{pmatrix}, \quad (3.10)$$

$$A2(s_2) = \begin{pmatrix} X_{U2}(s_2) \\ Y_{U2}(s_2) \end{pmatrix} = 2(\theta + s_2) \begin{pmatrix} \cos\left(s_2 - \frac{\varphi}{2}\right) \\ \sin\left(s_2 - \frac{\varphi}{2}\right) \end{pmatrix} - 4\sin\left(\frac{s_2}{2}\right) \begin{pmatrix} \cos\left(\frac{s_2}{2} - \frac{\varphi}{2}\right) \\ \sin\left(\frac{s_2}{2} - \frac{\varphi}{2}\right) \end{pmatrix}, \quad (3.11)$$

$$A3(s_3) = \begin{pmatrix} X_{U3}(s_3) \\ Y_{U3}(s_3) \end{pmatrix} = 2(\theta - s_3) \begin{pmatrix} \cos\left(s_3 + \frac{\varphi}{2}\right) \\ \sin\left(s_3 + \frac{\varphi}{2}\right) \end{pmatrix} + 4\sin\left(\frac{s_3}{2}\right) \begin{pmatrix} \cos\left(\frac{s_3}{2} + \frac{\varphi}{2}\right) \\ \sin\left(\frac{s_3}{2} + \frac{\varphi}{2}\right) \end{pmatrix}, \quad (3.12)$$

$$A6(s_6) = \begin{pmatrix} X_{U6}(s_6) \\ Y_{U6}(s_6) \end{pmatrix} = -4 \begin{pmatrix} \sin\left(\frac{\varphi}{2}\right) \\ 0 \end{pmatrix} + 4\sin\left(\frac{t_f + \varphi}{4}\right) \begin{pmatrix} \cos\left(\frac{-s_6}{2}\right) \\ \sin\left(\frac{-s_6}{2}\right) \end{pmatrix}. \quad (3.13)$$

The parameters  $s_1, s_2, s_3, s_6$  and the corresponding ranges of their changes are defined in (3.3) and (3.4).

Further analysis of the  $\varphi$ -sections of the reachable set  $G(t_f)$  will be carried out in the auxiliary coordinate system.



**3.4. The simplest properties of curves A1, A2, A3, and A6.** The curves A1 and A6 are arcs of circumferences. Each of them is symmetric w.r.t. the axis  $X$ , since the following relations are valid:

$$\begin{aligned} X_{U1}(s_1) &= X_{U1}(-s_1), & Y_{U1}(s_1) &= -Y_{U1}(-s_1); \\ X_{U6}(s_6) &= X_{U6}(-s_6), & Y_{U6}(s_6) &= -Y_{U6}(-s_6). \end{aligned}$$

The center of the circumference (the arc of which is the curve A1) coincides with the origin of the auxiliary system. The radius  $R_{A1}$  of the circumference is calculated using the formula

$$R_{A1} = 2\theta = t_f - \varphi. \quad (3.14)$$

The angular span of the arc A1 is equal to  $\varphi$ . Therefore, the curve A1 has no self-intersections for  $\varphi \in [0, 2\pi)$ . For  $\varphi \geq 2\pi$ , the curve A1 covers the entire circumference. The ‘‘overlap’’ points can be reached at different values of the parameter  $s_1$ , which differ by  $4\pi$ . If  $\varphi = 0$ , then the curve A1 degenerates to the point  $(t_f, 0)^\top$ . Let us denote by the symbol  $C_{A1}$  the circle of the radius  $R_{A1}$  with the center at the origin of the auxiliary coordinate system.

The center of the circumference, the arc of which is the curve A6, is located at the point

$$H = -4(\sin(\varphi/2), 0)^\top, \quad (3.15)$$

on the axis  $X$ . The radius  $R_{A6}$  of the circumference is equal to

$$R_{A6} = 4 \left| \sin((t_f + \varphi)/4) \right|. \quad (3.16)$$

Its value depends on  $t_f$ ,  $\varphi$  and becomes zero when  $(t_f + \varphi)$  is multiple of  $4\pi$ . The angular span of the arc A6 is equal to  $\theta$ . If  $(t_f + \varphi) < 4\pi$ , then  $\theta < 2\pi$  and the curve A6 has no self-intersections. We denote by the symbol  $C_{A6}$  the circle of the radius  $R_{A6}$  with the center at the point  $H$ .

The curves A2 and A3 are mutually symmetric w.r.t. the axis  $X$ . This property is defined by equalities

$$X_{U2}(s_2) = X_{U3}(s_3), \quad Y_{U2}(s_2) = -Y_{U3}(s_3) \quad (3.17)$$

that are valid for any parameter values  $s_2 = -s_3$  from ranges (3.4).

For controls of the type U3 forming the curve A3, let us analyze the degeneracy of the control constancy intervals. The first interval is non-degenerate for  $s_3 > 0$ , since we have  $t_1 = \varphi + s_3 > 0$  by virtue of (3.3) and (3.4). Duration of the second interval is determined by the formula  $t_2 - t_1 = t_f - \varphi - 2s_3$ . It vanishes only when  $s_3 = (t_1 - \varphi)/2 = \theta$ , i.e., at the last point of the curve A3. Duration of the third interval is  $t_f - t_2 = s_3$ . Therefore, the third interval degenerates only at the initial point of the curve A3. Thus, none of the control constancy intervals degenerates at the internal points of the curve A3. The similar property is true for the curve A2.

In Fig. 3, the curve A3 corresponding to  $\varphi = 0.3\pi$  and  $t_f = 2.7\pi$  is shown. The geometric method of constructing points  $A3(s_3)$  by controls of the type U3 is explained for several values of the parameter  $s_3$ . The motions leave the starting point  $o$  with the direction indicated by the arrow. On the interval  $[0, t_1)$ , each motion goes with  $u = +1$  along the dotted circumference counterclockwise. Then, it continues on the interval  $[t_1, t_2)$  by a straight-line motion with  $u = 0$ . The third interval  $[t_2, t_f]$  corresponds to the motion along the arc of the circumference with  $u = -1$  clockwise.



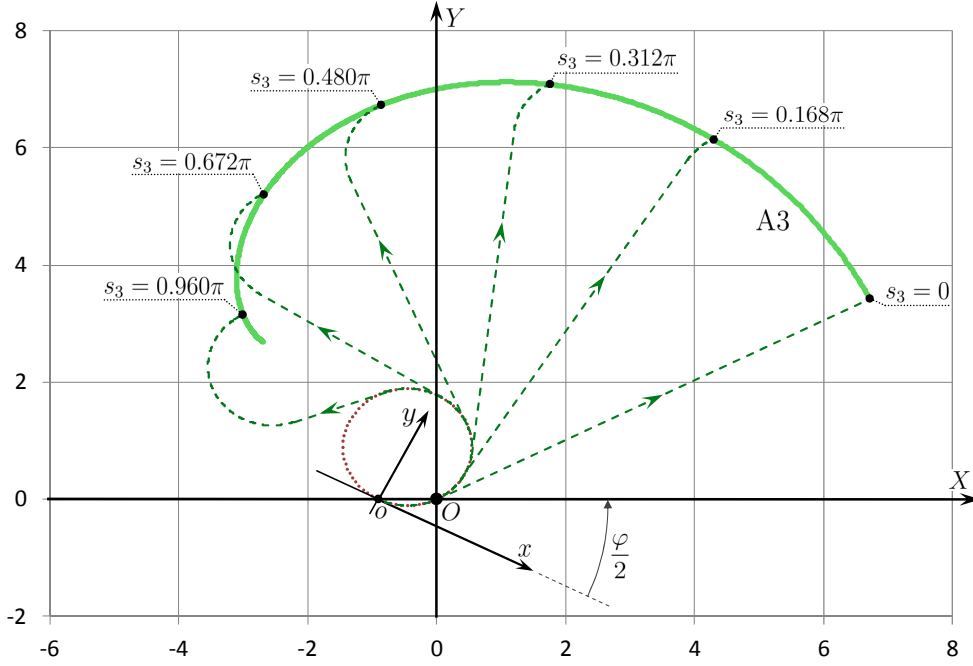


FIGURE 3. Formation of the curve A3 by means of controls of the type U3

Consider the curves A1, A2, A3, and A6 in the sequence A1, A3, A6, and A2 bypassing them in ascending parameters  $s_1, s_2, s_3$ , and  $s_6$ . For the extreme values of the parameters, we have

$$A1(s_1^e) = A3(s_3^b), \quad A3(s_3^e) = A6(s_6^b), \quad A6(s_6^e) = A2(s_2^b), \quad A2(s_2^e) = A1(s_1^b).$$

The listed docking points are denoted by  $\mathcal{P}_{1,3}$ ,  $\mathcal{P}_{3,6}$ ,  $\mathcal{P}_{2,6}$ , and  $\mathcal{P}_{1,2}$ . As a result of splicing, we get a continuous piecewise smooth closed curve, which we denote by the symbol  $A_\varphi(t_f)$ .

By virtue of Lemma 3.1, the boundary of the  $\varphi$ -section for  $\varphi \in [0, t_f)$  is a subset of the curve  $A_\varphi(t_f)$ . When selecting parts of the curves A1, A3, A6, and A2 that form the boundary of the  $\varphi$ -section, significant difficulty is caused by presence of self-intersections of the curve  $A_\varphi(t_f)$ .

In Fig. 4, two examples of the curve  $A_\varphi(t_f)$  are given. The docking points of the curves A1, A3, A6, and A2 are marked with risks. For the values  $t_f = 3\pi$  and  $\varphi = 0.4\pi$  (Fig. 4a), the curve  $A_\varphi(t_f)$  has no self-intersections. There are many self-intersection points for the values  $t_f = 10\pi$  and  $\varphi = 0.4\pi$  (Fig. 4b). When changing  $s_6$  in the range  $[-\theta, \theta]$ , the points  $A6(s_6)$  go along the boundary of the circle  $C_{A6}$  clockwise from the point of docking with the curve A3 to the point of docking with the curve A2. Herewith, on Fig. 4b, the point  $A6(s_6)$  makes more than two turns.

Structure of the curve  $A_\varphi(t_f)$  (for a fixed  $\varphi$ ) becomes more complicated with the growth of  $t_f$ .

Further in this section, location of the curves A1, A2, A3, and A6 in the plane  $X, Y$  will be investigated.

**3.5. Curves A2 and A3 are parts of circle's involutes.** Each of the curves A2 and A3 is some part of the involute of the circle. We show it for the curve A2. Let us rewrite equation (3.11)

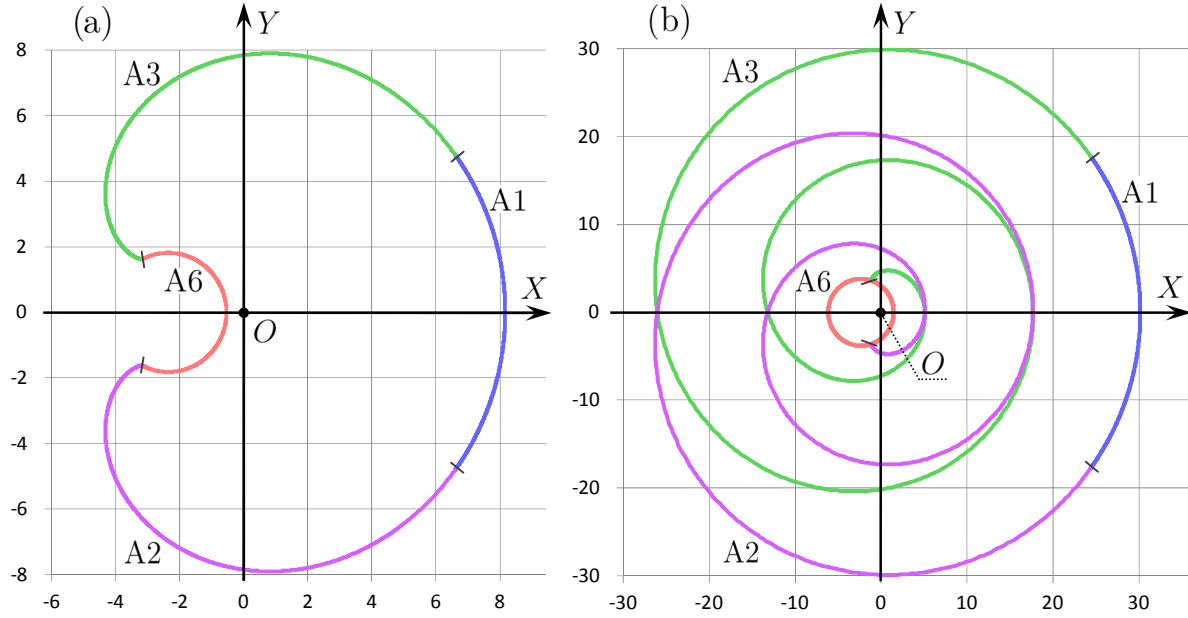


FIGURE 4. The curve  $A_\varphi(t_f)$  for  $t_f = 3\pi$ ,  $\varphi = 0.4\pi$  (a), and  $t_f = 10\pi$ ,  $\varphi = 0.4\pi$  (b)

for the curve A2 in the equivalent form using the trigonometric transformation of the last term:

$$A2(s_2) = 2(\theta + s_2) \begin{pmatrix} \cos\left(s_2 - \frac{\varphi}{2}\right) \\ \sin\left(s_2 - \frac{\varphi}{2}\right) \end{pmatrix} + 2 \begin{pmatrix} -\sin\left(s_2 - \frac{\varphi}{2}\right) \\ \cos\left(s_2 - \frac{\varphi}{2}\right) \end{pmatrix} - 2 \begin{pmatrix} \sin\left(\frac{\varphi}{2}\right) \\ \cos\left(\frac{\varphi}{2}\right) \end{pmatrix}. \quad (3.18)$$

The canonical form of the parametric representation of the involute of a circle is taken in the following form (see [45, p. 252, formula (1)], [46, §11, p. 43]):

$$\begin{aligned} x_1 &= r \cos \tau + r\tau \sin \tau, \\ x_2 &= r \sin \tau - r\tau \cos \tau. \end{aligned} \quad (3.19)$$

Here,  $x_1$  and  $x_2$  are the rectangular coordinates,  $\tau \geq 0$  is a parameter. The radius of the base circle is  $r$ , its center is located at the origin. The involute at  $\tau = 0$  leaves the point  $(0, r)^\top$ .

Let us represent the curve A2, given by formula (3.18), in form (3.19) using the rotation and shift operations. The shift is provided by the third term in (3.18), it does not depend on  $s_2$ . Next, we shall replace the variables  $\tau = \theta + s_2$ ,  $\tau \in [0, \theta]$ . After that, the first two terms in (3.18) (after rearranging them) will be written as follows:

$$2 \begin{pmatrix} -\sin\left(\tau - \theta - \frac{\varphi}{2}\right) \\ \cos\left(\tau - \theta - \frac{\varphi}{2}\right) \end{pmatrix} + 2\tau \begin{pmatrix} \cos\left(\tau - \theta - \frac{\varphi}{2}\right) \\ \sin\left(\tau - \theta - \frac{\varphi}{2}\right) \end{pmatrix}. \quad (3.20)$$

Further, we introduce the rotation matrix

$$\begin{pmatrix} \cos \psi & \sin \psi \\ -\sin \psi & \cos \psi \end{pmatrix}$$

and multiply it by vector (3.20). Assuming  $\psi = \frac{\pi}{2} - \theta - \frac{\varphi}{2}$ , we get for (3.20) representation of form (3.19):

$$2 \begin{pmatrix} \cos \tau \\ \sin \tau \end{pmatrix} + 2\tau \begin{pmatrix} \sin \tau \\ -\cos \tau \end{pmatrix}.$$

Thus, the curve A2 is the initial part of the circle's involute. As a result, it does not have self-intersections. The center of the base circle is located at the point  $2(-\sin(\varphi/2), -\cos(\varphi/2))^T$ , its radius is 2. The starting point of the involute corresponds to the value  $s_2 = -\theta$ .

The curve A3 is symmetric to the curve A2 and, also, represents the initial part of the involute of the circle. For it, the radius of the base circle is the same as for the curve A2, and its center is located at the point  $2(-\sin(\varphi/2), \cos(\varphi/2))^T$  symmetrically w.r.t. the axis X.

Note that the point  $O$  of the auxiliary system  $X, Y$  origin always belongs to both base circles.

In Fig. 5 for  $t_f = 2.5\pi$  and  $\varphi = \pi/3$ , the base circles corresponding to the involutes A3 and A2 are shown. Dotted straight lines generate points of the curve A3 (of the curve A2, respectively) as the points of the circle's involute. Curves A1 and A6 are also presented.

We emphasize that the dotted lines (coming to the curve A3 or the curve A2) are not the trajectories of the system (2.1) from the initial phase point  $x_0 = y_0 = \varphi_0 = 0$  and do not satisfy the boundary condition for  $\varphi$  when hitting the curve A3 or the curve A2.

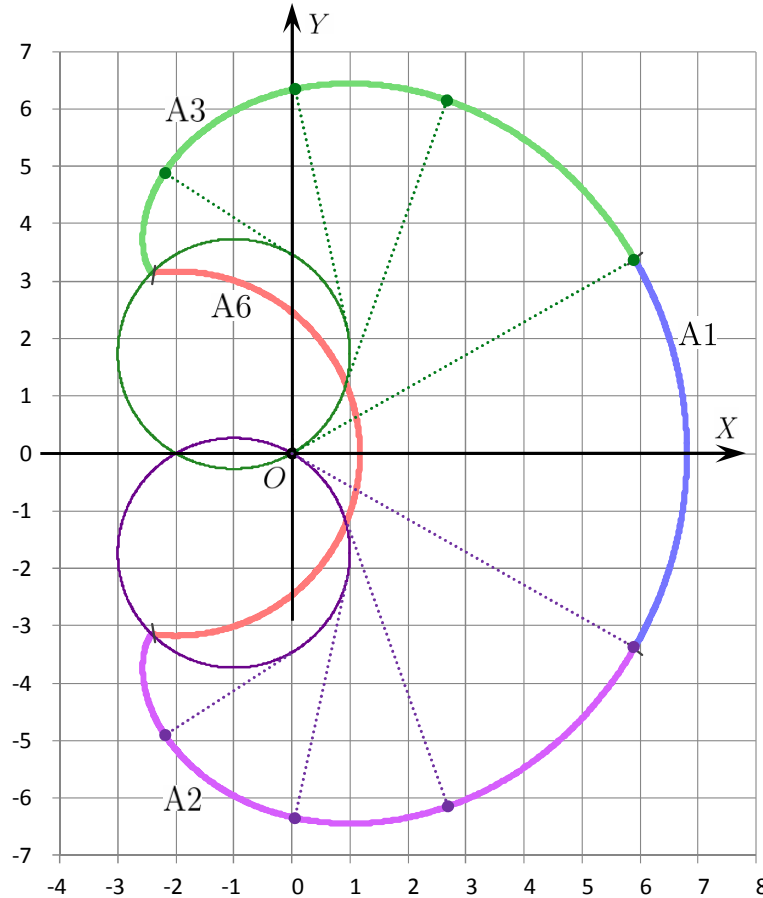


FIGURE 5. Representation of the curves A3 and A2 in the form of involutes

**3.6. Mutual arrangement of curves A1, A2, A3, and A6.** Denote by the symbol  $R_{1,6}(s_6)$  the distance from the center of the curve A1 (it coincides with the origin  $O$  of the auxiliary system) to the points of the curve A6. Let  $R_{6,1}(s_1)$ ,  $R_{6,2}(s_2)$ , and  $R_{6,3}(s_3)$  be respectively distances from the center  $H$  of the curve A6 to the points of the curves A1, A2, and A3.

The denotations used here are illustrated in Fig. 6. Calculations are made for  $t_f = 2.4\pi$  and  $\varphi = 0.8\pi$ .

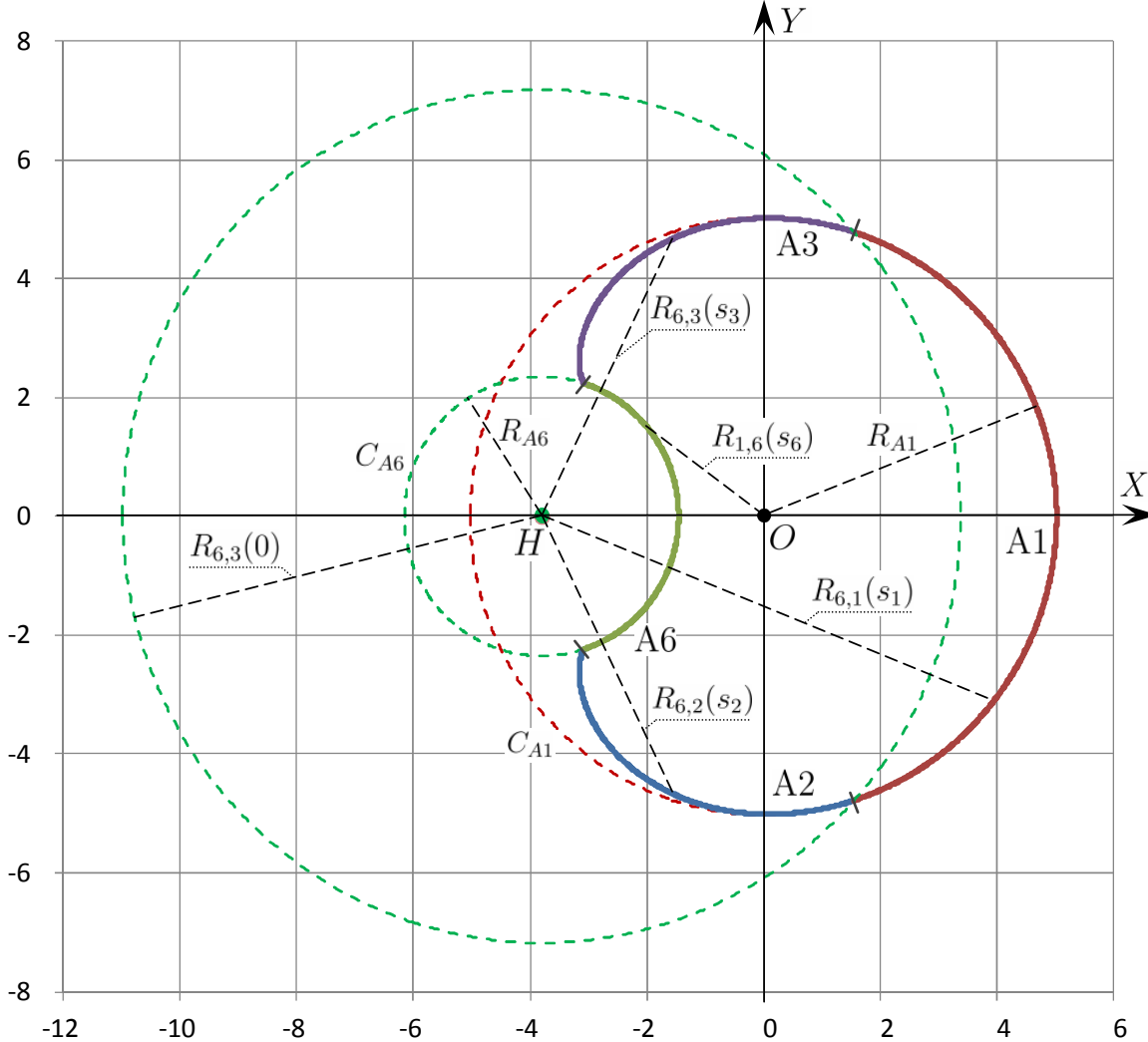


FIGURE 6. Explanation of denotations for the study of the mutual arrangement of the curves A1, A2, A3, and A6

1) Let us start with analysis of the relative arrangement of the curves A1 and A6. We show that the following relation

$$(R_{A1})^2 - (R_{1,6}(s_6))^2 > 0, \quad s_6 \in [s_6^b, s_6^e] = [-\theta, \theta] \quad (3.21)$$

is fulfilled. Therefore, the curve A6 belongs to  $\text{int}C_{A1}$ .

By virtue of formulas (3.10) and (3.13), we get  $(R_{A1})^2 - (R_{1,6}(s_6))^2 = 4D_{1,6}(s_6)$ ,

where

$$D_{1,6}(s_6) = \theta^2 - 4 \sin^2 \left( \frac{\varphi}{2} \right) + 8 \sin \left( \frac{\varphi}{2} \right) \sin \left( \frac{\varphi + \theta}{2} \right) \cos \left( \frac{s_6}{2} \right) - 4 \sin^2 \left( \frac{\varphi + \theta}{2} \right).$$

The sign of inequality (3.21) is defined by the expression for  $D_{1,6}(s_6)$ .

It can be seen that  $D_{1,6}(s_6) > 0$  if  $\theta > 4$ . Now let  $0 < \theta \leq 4$ . Given the range of the values  $s_6$ , we have  $-2 \leq -\theta/2 \leq s_6/2 \leq \theta/2 \leq 2$ . Therefore,  $\cos(\theta/2) \leq \cos(s_6/2) \leq \cos(0) = 1$ . The expression  $\cos(s_6/2)$  is included linearly in the definition of the function  $D_{1,6}(s_6)$ . So, its minimum is reached either at  $s_6 = 0$ , or at  $s_6 = \pm\theta$ . Taking into account the parity of the function  $D_{1,6}(s_6)$ , the condition  $D_{1,6}(s_6) > 0$  needs to be checked only for two values  $s_6 = 0$  and  $s_6 = \theta$ .

Using trigonometric transformations, we obtain

$$\begin{aligned} D_{1,6}(0) &= \theta^2 - 4 \sin^2 \left( \frac{\varphi}{2} \right) + 8 \sin \left( \frac{\varphi}{2} \right) \sin \left( \frac{\varphi + \theta}{2} \right) - 4 \sin^2 \left( \frac{\varphi + \theta}{2} \right) \\ &= \theta^2 - 4 \sin^2 \left( \frac{\theta}{2} \right) = 4 \left( \left( \frac{\theta}{2} \right)^2 - \sin^2 \left( \frac{\theta}{2} \right) \right) > 0, \\ D_{1,6}(\theta) &= \theta^2 - 4 \sin^2 \left( \frac{\varphi}{2} \right) + 8 \sin \left( \frac{\varphi}{2} \right) \sin \left( \frac{\varphi + \theta}{2} \right) - \cos \left( \frac{\theta}{2} \right) - 4 \sin^2 \left( \frac{\varphi + \theta}{2} \right) \\ &= \theta^2 - 4 \left( \sin \left( \frac{\varphi}{2} \right) - \sin \left( \frac{\varphi + \theta}{2} \right) \right)^2 \\ &= \theta^2 - 4 \left( 2 \sin \left( \frac{\theta}{4} \right) \cos \left( \frac{\theta}{4} + \frac{\varphi}{2} \right) \right)^2 > \theta^2 - 16 \sin^2 \left( \frac{\theta}{4} \right) > 0. \end{aligned}$$

Thus, for  $\varphi \in [0, t_f)$ , the inequality  $D_{1,6}(s_6) > 0$  is satisfied for all  $s_6 \in [s_6^b, s_6^e] = [-\theta, \theta]$ . This means that  $A_6 \subset \text{int}C_{A1}$ . As a consequence, we see that the arcs  $A_1$  and  $A_6$  have no common points.

2) Let describe the docking of the curves  $A_2$  and  $A_3$  with the curve  $A_1$ .

The radius of curvature of the involute at the current point is the distance from it along the generating straight line to the point of contact of the line with the base circle [45, p. 252].

For the involute  $A_3$  at the current value of the parameter  $s_3$ , the point of contact of the generating straight line with the base circle is a vector representing the second term in the right part of formula (3.12). The radius of curvature of the curve  $A_3$  at the current point is the modulus of the first term in (3.12), *i.e.*,  $2(\theta - s_3)$ . For the starting point of the curve  $A_3$  (where  $s_3 = 0$ ), the point of tangency of the generating straight line with the base circle coincides with the origin of the coordinates of the plane  $X, Y$ , and the radius of curvature is  $2\theta$ . The circumference, on which the arc  $A_1$  lies, has the same center and the same radius. Consequently, the curves  $A_1$  and  $A_3$  are smoothly joined with the coincidence of curvature. Since the radius of curvature of the involute  $A_3$  monotonically decreases with the growth of  $s_3$ , the entire curve  $A_3$  (excepting the starting point) belongs to  $\text{int}C_{A1}$  [47, Theorem 2]. It follows that the curves  $A_1$  and  $A_3$  have only one common point (*i.e.*, the junction point  $\mathcal{P}_{1,3}$ ).

Similarly, due to symmetry, the curve  $A_2$  (excepting the point  $\mathcal{P}_{1,2}$  that is the point of junction with the curve  $A_1$ ) belongs to  $\text{int}C_{A1}$ .

3) To estimate the relative location of the curves A2 and A6, consider the function  $s_2 \rightarrow (R_{6,2}(s_2))^2$ . Based on (3.11) and (3.13), we have

$$(R_{6,2}(s_2))^2 = 4 \left( (\theta + s_2)^2 + \left(2 \sin\left(\frac{s_2}{2}\right)\right)^2 + \left(2 \sin\left(\frac{\varphi}{2}\right)\right)^2 - 4(\theta + s_2) \sin\left(\frac{s_2}{2}\right) \cos\left(\frac{s_2}{2}\right) + 4(\theta + s_2) \cos\left(s_2 - \frac{\varphi}{2}\right) \sin\left(\frac{\varphi}{2}\right) - 8 \sin\left(\frac{s_2}{2}\right) \cos\left(s_2 - \frac{\varphi}{2}\right) \sin\left(\frac{\varphi}{2}\right) \right).$$

Substituting  $s_2 = s_2^b = -\theta$ , we get

$$(R_{6,2}(-\theta))^2 = 4 \left( 2 \sin\left(\frac{\varphi + \theta}{2}\right) \right)^2 = (R_{A6})^2.$$

Let us express the derivative of the function  $(R_{6,2}(s_2))^2$  with respect to the parameter  $s_2$ :

$$\left( (R_{6,2}(s_2))^2 \right)'_{s_2} = 8(\theta + s_2) \left( 1 - \cos(s_2) - 2 \sin\left(s_2 - \frac{\varphi}{2}\right) \sin\left(\frac{\varphi}{2}\right) \right).$$

After trigonometric transformations, we have

$$\left( (R_{6,2}(s_2))^2 \right)'_{s_2} = 8(\theta + s_2) (1 - \cos(s_2 - \varphi)) \geq 0.$$

The resulting inequality turns into the equality only in a finite number of values of the parameter  $s_2$ . Therefore, the function  $(R_{6,2}(s_2))^2$  is strictly monotonically increasing in the parameter  $s_2$ . Thus, for  $\varphi < t_f$ , the inequality  $R_{6,2}(s_2) > R_{A6}$  is valid for all  $s_2 \in (s_2^b, s_2^e]$ . The similar inequality  $R_{6,3}(s_3) > R_{A6}$  is also fulfilled for the points of the curve A3.

4) Let  $0 \leq \varphi < 2\pi$ . Let us show that the curve A1 lies outside the interior of the circle, whose center is at the point  $H$  (Fig. 6) and the radius is the distance from the point  $H$  to the points  $\mathcal{P}_{1,3}$  and  $\mathcal{P}_{1,2}$ .

The square of the distance from the point  $H$  to the junction point of the curves A1 and A3 can be calculated by the formula

$$(R_{6,3}(s_3 = 0))^2 = 4 \left( \theta^2 + \left(2 \sin\frac{\varphi}{2}\right)^2 + 2\theta \sin\varphi \right).$$

The square of the distance from the point  $H$  to the points of the curve A1 is found by the formula

$$\begin{aligned} (R_{6,1}(s_1))^2 &= \left( X_{U1}(s_1) + 4 \sin\left(\frac{\varphi}{2}\right) \right)^2 + (Y_{U1}(s_1))^2 \\ &= \left( 2\theta \cos\frac{s_1}{2} \right)^2 + 16\theta \cos\frac{s_1}{2} \sin\frac{\varphi}{2} + \left( 4 \sin\frac{\varphi}{2} \right)^2 + \left( 2\theta \sin\frac{s_1}{2} \right)^2. \end{aligned}$$

Consider the difference

$$(R_{6,1}(s_1))^2 - (R_{6,3}(0))^2 = 16\theta \cos\frac{s_1}{2} \sin\frac{\varphi}{2} - 8\theta \sin\varphi = 16\theta \sin\frac{\varphi}{2} \left( \cos\frac{s_1}{2} - \cos\frac{\varphi}{2} \right).$$

Taking into account the inequalities  $-\pi < -\varphi/2 \leq s_1/2 \leq \varphi/2 < \pi$  and the cosine properties, we obtain that the last factor of the written difference (like the difference itself) cannot be less than zero.

Therefore, the minimum distance from the point  $H$  to the points of the curve A1 is achieved at the points  $\mathcal{P}_{1,3}$  and  $\mathcal{P}_{1,2}$ , i.e.,  $R_{6,1}(-\varphi) = R_{6,1}(\varphi) \leq R_{6,1}(s_1)$  for any  $s_1 \in [-\varphi, \varphi]$ .

5) Let us prove that the curves A2 and A3 can intersect only at points on the axis  $X$ .

Suppose the contrary, that there is a point of intersection of the curves A2 and A3 lying outside the axis  $X$ . Let this point correspond to some values of the parameters  $\tilde{s}_2$  and  $\tilde{s}_3$ . The curves A2 and A3 are symmetric w.r.t. the axis  $X$ . Therefore, there is a point on the curve A3 corresponding to some parameter  $\hat{s}_3$ , for which  $X_{U3}(\hat{s}_3) = X_{U2}(\tilde{s}_2)$ ,  $Y_{U3}(\hat{s}_3) = -Y_{U2}(\tilde{s}_2)$ . Since  $Y_{U3}(\hat{s}_3) = -Y_{U3}(\tilde{s}_3) \neq 0$ , then  $\hat{s}_3 \neq \tilde{s}_3$ . Thus, two different points were obtained on the curve A3 that are symmetric w.r.t. the axis  $X$ . Therefore, they are equally distanced from any point on the axis  $X$ , in particular, from the point  $H$ . Above, the strict monotony of changing the distance from the point  $H$  to the points of the curve A3 was established. Therefore, the points of the curve A3 specified by the parameters  $\tilde{s}_3$  and  $\hat{s}_3$  have different distances to the point  $H$ . We came to the contradiction.

**3.7. List of properties of curves A1, A2, A3, and A6.** Let us summarize the properties of the curves A1, A2, A3, and A6 in the plane  $X, Y$  at  $0 \leq \varphi < t_f$ .

1. Each of the curves A1 and A6 is symmetric w.r.t. the axis  $X$  and is an arc of the circumference, whose center lies on the axis  $X$ . The span of the arc can be greater than  $2\pi$ . The curve A1 degenerates to a point only when  $\varphi = 0$ . The curve A6 degenerates to a point only when  $(t_f + \varphi)$  is multiple to  $4\pi$ .

2. Each of the curves A2 and A3 represents the initial part of the involute of the circle, therefore, it does not have self-intersections.

3. The curves A2 and A3 are mutually symmetric w.r.t. the axis  $X$  and can intersect only at points on this axis.

4. All internal points of the curve A2 (respectively, A3) are generated by controls of the type U2 (U3) with three non-degenerate constancy intervals.

5. The distance  $R_{6,2}(s_2)$  from the center  $H$  of the circle  $C_{A6}$  to the point on the curve A2 (defined by the parameter  $s_2$ ) increases monotonically as the parameter  $s_2$  grows.

6. The distance  $R_{6,3}(s_3)$  from the center  $H$  of the circle  $C_{A6}$  to the point on the curve A3 (defined by the parameter  $s_3$ ) decreases monotonically as the parameter  $s_3$  grows.

7. The curves A2 and A3 are smoothly mated with the curve A1. The radii of curvature at the docking points are the same.

8. The curves A2 and A3 (excepting the points of their junction with the curve A1) as well as the entire curve A6 lie in the interior of the circle  $C_{A1}$ .

9. The curves A2 and A3 (excepting the points of their junction with the curve A6) lie outside the circle  $C_{A6}$ .

10. For  $\varphi \in [0, 2\pi)$ , the distance from the center  $H$  of the circle  $C_{A6}$  to the curve A1 is achieved at the curve extreme points.

11. Connection of the curves A1, A2, A3, and A6 forms a piecewise smooth closed curve that is symmetric w.r.t. the axis  $X$ .

#### 4. AUXILIARY STATEMENTS ABOUT EXTREME MOTIONS LEADING TO THE INTERIOR OF THE REACHABLE SET $G(t_f)$

Paper [40] contained statements characterizing the extreme motions leading to the interior of the reachable set  $G(t_f)$ . In this paper, additional statements on this topic will be required. When considering them, we shall use the following important property [40, 43]. Let some control  $u^*(\cdot)$  and the corresponding motion  $z^*(\cdot)$  of system (2.1) satisfy the PMP. Then, if the control  $u^*(\cdot)$  has more than two switch instants, then the geometric positions of  $(x^*(t), y^*(t))^T$  at these instants



lie on a single straight line, which is called the switching one. Also, if the control  $u^*(\cdot)$  has an interval with  $u^*(t) \equiv 0$ , then the corresponding part of the rectilinear motion in the plane  $x, y$  lies on the straight switch line.

Now we prove two statements about extreme motions with cycles. By a cycle, we mean a part of motion with the constant control  $u = \pm 1$  and the length greater or equal to  $2\pi$ .

**Lemma 4.1.** *Let a motion  $z(\cdot)$  of system (2.1) with  $\varphi(t_f) \geq 0$  be generated by a control of the type U2 or U3 with three non-degenerate control constancy intervals. If at least one of these two extreme intervals has duration of at least  $2\pi$ , then  $z(t_f) \in \text{int}G(t_f)$ .*

*Proof.* From the assumption of two extreme time intervals of control constancy, the presence of a “cycle” on at least one of them follows.

Consider a control  $u(\cdot)$  of the type U3:  $u(t) = 1$  on the interval  $t \in [0, t_1)$ ,  $u(t) = 0$  for  $t \in [t_1, t_2)$ , and  $u(t) = -1$  on the interval  $t \in [t_2, t_f)$ . Since  $\varphi(t_f) \geq 0$ , the presence of a cycle on the third interval entails the presence of a cycle on the first interval. Therefore, it is sufficient to consider the presence of a cycle only on the first interval (Fig. 7a), i.e.,  $t_1 \geq 2\pi$ . Take the instant  $\hat{t} \in (t_2, t_f)$  so that  $\hat{t} - t_2 < 2\pi$ . Let us construct an additional motion  $\tilde{z}(\cdot)$  with the control

$$\tilde{u}(t) = \begin{cases} 1, & t \in [t_0, t_1 - 2\pi), \\ 0, & t \in [t_1 - 2\pi, t_2 - 2\pi), \\ -1, & t \in [t_2 - 2\pi, \hat{t} - 2\pi), \\ 1, & t \in [\hat{t} - 2\pi, \hat{t}), \\ -1, & t \in [\hat{t}, t_f]. \end{cases}$$

Such a motion comes at the instant  $t_f$  to the same point and with the same value  $\varphi$  as the original motion (Fig. 7). At the same time, the additional motion at the switch instant  $\hat{t}$  does not lie on the switch line (along which the motion goes at  $u = 0$ ). Thus, PMP will not be performed for the additional motion. Therefore,  $z(t_f) \in \text{int}G(t_f)$ .

For the curve A2, the statement is true due to the symmetry of the curves A2 and A3.  $\square$

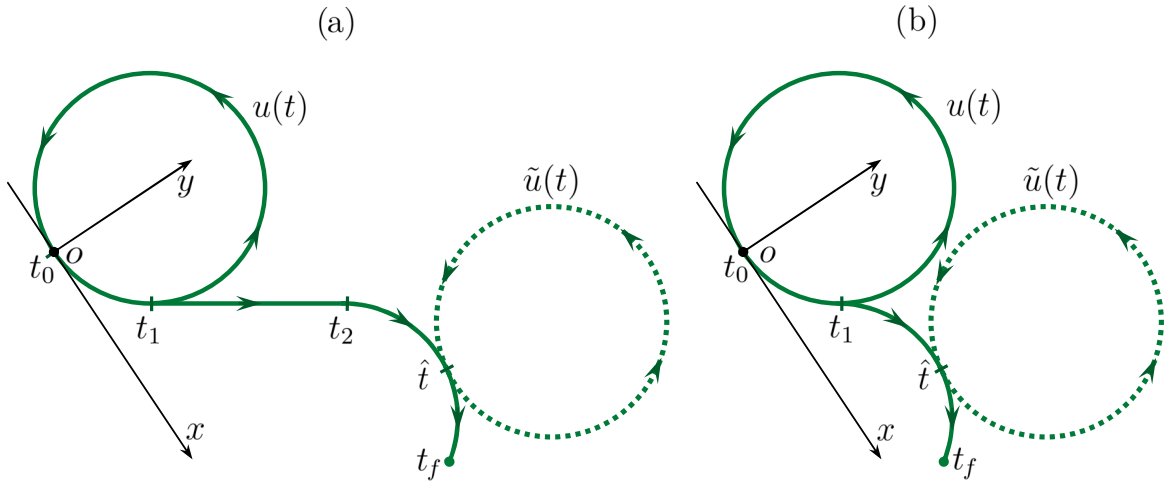


FIGURE 7. Illustration for the proofs of Lemmas 4.2 and 4.3

**Lemma 4.2.** *Let a motion  $z(\cdot)$  of system (2.1) be generated by a control of the type U6. Wherein, some two adjacent intervals of the control constancy are non-degenerate. If at least one of them has duration greater than  $2\pi$ , then  $z(t_f) \in \text{int}G(t_f)$ .*

*Proof.* By assumption, we have a cyclic motion with a duration greater than  $2\pi$  on one of two non-degenerate adjacent parts (with constant control) of the original motion  $z(\cdot)$ . We transfer a cycle of duration  $2\pi$  from this part to any interior point of a non-degenerate neighboring part. We get an additional motion  $\tilde{z}(\cdot)$  going to the same phase point at the time  $t_f$  as the original motion  $z(\cdot)$ . Additional motion has at least four consecutive non-degenerate parts of control constancy with values of  $\pm 1$ , i.e., at least three switch instants. Due to Lemma 3 from [40], the additional motion leads to the point  $\tilde{z}(t_f) \in \text{int}G(t_f)$ . Therefore,  $z(t_f) \in \text{int}G(t_f)$ .

The proof is illustrated in Fig. 7b. Here, for the original motion, the first and second intervals of control constancy are non-degenerate. The cycle is located on the first interval. This cycle is carried over to the second motion part to the point  $(x(\hat{t}), y(\hat{t}))^\top$  of the original motion. We get the additional motion with three switch instants.  $\square$

The proof of the next statement is the longest.

**Lemma 4.3.** *Let a motion  $z(\cdot)$  be generated by a control of the type U3 and lead to the point  $z(t_f) = (x(t_f), y(t_f), \varphi(t_f))^\top$ , for which  $\varphi(t_f) \geq 0$ . Suppose that for the point  $(x(t_f), y(t_f))^\top$  after transferring it to the auxiliary system  $X, Y$ , the inequality  $Y(t_f) < 0$  is fulfilled. In addition, it is assumed that all three time intervals of constancy of the control are non-degenerate, and the duration of both the first and third intervals is less than  $2\pi$ . Then  $z(t_f) \in \text{int}G(t_f)$ .*

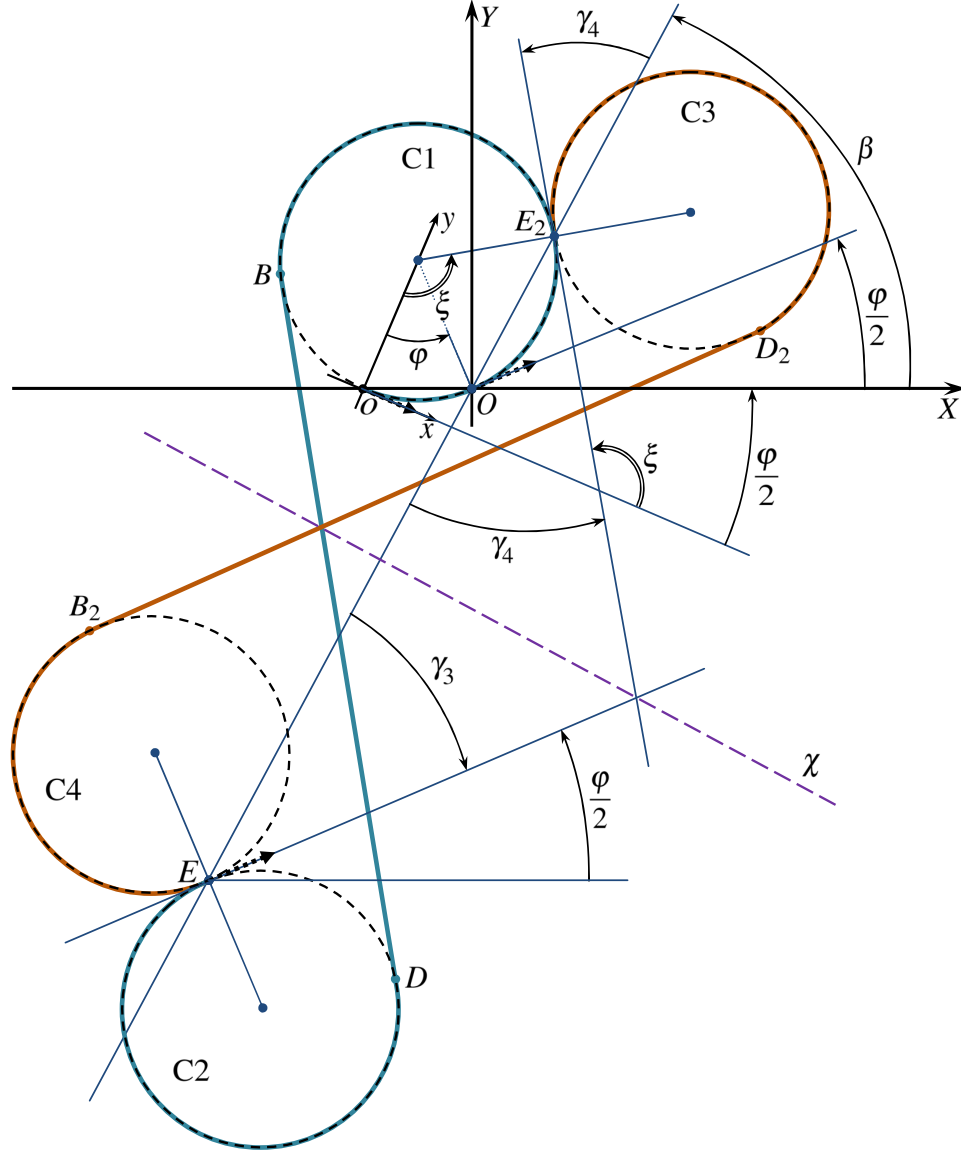
*Proof.* Let  $E$  be the geometric position of the motion at the instant  $t_f$ . The method of proof will be as follows. Together with the original motion leading to the point  $E$  for the given value  $\varphi$  at the instant  $t_f$ , we shall construct an additional motion leading from the same starting point to the point  $E$  for the same values  $\varphi$  and  $t_f$ . The additional motion could be built in such a way that the PMP will not be performed for it. Consequently,  $z(t_f) \in \text{int}G(t_f)$ .

1) By assumption, the control of the type U3 has three non-degenerate time intervals with the values  $1, 0, -1$ . The points of the geometric position at the switch instants  $t_1$  and  $t_2$  are denoted by  $B$  and  $D$  (Figs. 8–10). The circumference along which the motion goes on the interval  $[0, t_1]$  will be called the first (marked by the symbol C1), and the circumference with the motion on the interval  $[t_2, t_f]$  is called the second (marked by the symbol C2). The original coordinate system is denoted by  $x, y$ , the auxiliary one is denoted by  $X, Y$ . The point  $O$  is the origin of the auxiliary system. The axis  $X$  of the auxiliary system passes through the starting point of the motion and constitutes an angle  $\varphi/2$  with the direction of the axis  $x$ . The angle is counted counterclockwise from the axis  $x$ . The point  $E$  is assumed to be below the axis  $X$ . The direction vector of the motion at the points  $O$  and  $E$  makes the angle  $\varphi/2$  with the axis  $X$  (counted from the axis  $X$  counterclockwise).

2) Since  $\varphi \geq 0$  and the original motion is a motion of the type U3, then  $t_1 \geq \varphi$ . For the instant  $t = \varphi$ , the corresponding geometric position in the coordinates  $x, y$  is described by the relation  $(x(t), y(t))^\top = (\sin \varphi, 1 - \cos \varphi)^\top$ . From formula (3.9), it is seen that such a point coincides with the point  $O$ .

Consider the straight line  $EO$  with the direction from  $E$  to  $O$ . Let  $\beta$  be the angle between this straight line and the axis  $X$ . This angle is counted counterclockwise from the axis  $X$ . Since the




 FIGURE 9. Additional motion for the condition  $\beta > \varphi/2$ 

obtained by virtue of the control of the type U3. The inequality  $t_1 < 2\pi$  is satisfied due to the assumption that there are no cycles on the original motion. Considering additionally that the point  $E$  lies below the axis  $X$ , we obtain the range of admissible values of  $\alpha$  in the form  $(0, 2\pi - \varphi/2)$ .

Let us show that  $\alpha > \beta$ . Indeed, the point  $E$  does not coincide with the point  $D$ , since on the original motion there are no degenerate time intervals of constant control and there are no cycles. Hence,  $E \neq K$  and  $E \neq O$ . Therefore, the angles  $\gamma_1$  and  $\gamma_2$  are uniquely defined, and the inequalities  $\gamma_1 \geq 0$  and  $\gamma_2 > 0$  are satisfied. In addition, one can see from Fig. 10 that  $\alpha = \beta + \gamma_1 + \gamma_2$ . So, it follows that  $\alpha > \beta$ .

The angle  $\alpha$  can be calculated by the formula  $\alpha = t_1 - \pi - \varphi/2$  (see Fig. 10). From the inequality  $\alpha > \beta$ , we get  $t_1 - \pi - \varphi/2 > \beta$ . Since  $\varphi \geq 0$  and  $0 < \beta < \pi$ , we have



relatively to the straight line  $\chi$ . Namely, in the time interval from  $t_1^*$  to  $t_2^* = 2\beta + t_f - t_2$ , the additional motion goes with the control  $u = -1$  along the circumference C3 clockwise from the point  $E_2$  to the point  $D_2$ . In the interval from  $t_2^*$  to  $t_3^* = 2\beta + t_f - t_1$ , the motion proceeds with zero control along the straight line segment of the length  $t_3^* - t_2^* = t_2 - t_1$  from the point  $D_2$  to the point  $B_2$ . The final stage of the motion from the instant  $t_3^*$  to the instant  $t_f$  occurs with the control  $u = 1$  along the circumference C4 counterclockwise from the point  $B_2$  to the point  $E$ . The constructed curve leads to the same point  $E$  and with the same direction  $\varphi$  as the original one. Its length coincides with the length of the original curve.

According to the assumption, there are three non-degenerate intervals of the control constancy on the original motion, and there are no cycles on the first and third time intervals. Considering the inequality  $t_1 > 2\beta > 0$ , we get that there are three switch instants on the additional motion that satisfy the inequalities  $0 < t_1^* < t_2^* < t_3^* < t_f$ . At the same time, there are no cycles in the second interval of the control constancy (motion from the point  $E_2$  to the point  $D_2$ ). From this, it follows that the points of the geometric position of the additional motion at the switch instants do not lie on the same straight line. The latter contradicts to the PMP. Therefore,  $z(t_f) \in \text{int}G(t_f)$ .  $\square$

**Remark 4.4.** Figures 8-10 (explaining the proof of Lemma 4.3) are made for  $0 < \varphi < \pi$ . If  $\varphi = 0$ , then we consider only the variant  $\beta > \varphi/2 = 0$ . All elements of the proof based on Fig. 9 are preserved. If  $\pi \leq \varphi < 2\pi$ , then we are dealing only with the variant  $\beta < \varphi/2$ . This follows from the fact that the inequality  $\beta < \pi/2$  is satisfied. Indeed, for  $\beta \geq \pi/2$ , duration of the first time interval of control constancy exceeds  $2\pi$ . It contradicts the assumption that there are no cycles on the original motion. When analyzing the variant  $\beta < \varphi/2$ , all elements of the proof that were made with reference to Fig. 8 are preserved.

## 5. STATEMENTS ABOUT THE STRUCTURE OF $\varphi$ -SECTIONS

Proofs of Lemmas 5.1 and 5.2 formulated below are based on the Jordan curve theorem [48, 49], which characterizes partition of the plane by a continuous closed curve  $S$  without self-intersections. According to the Jordan theorem, the set  $\mathbb{R}^2 \setminus S$  consists of two open, connected and disjoint components  $S^+$  (external unlimited) and  $S^-$  (internal limited). The curve  $S$  is the boundary of these components.

Lemmas 5.1 and 5.2 are used later to construct the boundary of the  $\varphi$ -sections. Lemma 5.3 will also be used in the sequel.

**Lemma 5.1.** *Consider some values  $t_f > 0$  and  $\varphi \in [0, t_f)$ . Let  $S$  be a continuous closed curve without self-intersections in the plane  $x, y$ , and to any point of  $S$  at least one of the controls of the types U1, U2, U3, and U6 leads at the instant  $t_f$  (with the given value  $\varphi$ ). Suppose that the set  $S^+$  contains no points formed by controls of the types U1, U2, U3, and U6 for the mentioned values  $t_f$  and  $\varphi$ . Then  $S \subset \partial G_\varphi(t_f)$  and*

$$G_\varphi(t_f) \cap S^+ = \emptyset. \quad (5.1)$$

*Proof.* Let us show that relation (5.1) holds. On the contrary, let the set  $S^+$  contain some point  $P \in G_\varphi(t_f)$ . The reachable set  $G(t_f)$  of system (2.1), and, therefore, its section  $G_\varphi(t_f)$  are bounded. Let us choose in the unlimited set  $S^+$  some point  $Q \notin G_\varphi(t_f)$ . We connect the points

$P$  and  $Q$  by a continuous curve  $\gamma$  that lies entirely in  $S^+$ . It is possible due to the connectedness of the set  $S^+$ . By virtue of continuity, the curve  $\gamma$  contains a point  $E \in \partial G_\varphi(t_f)$ . According to Lemma 3.1, at least one of the controls of the type U1, U2, U3, U6 leads to the point  $E$ . But it is impossible by the hypothesis of the lemma being proved. Therefore,  $E \notin \partial G_\varphi(t_f)$ . We came to a contradiction, i.e., the initial assumption that  $P \in G_\varphi(t_f)$  is wrong. Thus, relation (5.1) is established.

We have  $S = \partial S^+$  and (by the condition of this lemma) for any point of the curve  $S$ , some admissible control exists leading to this point. Taking into account (5.1), we get that  $S \subset \partial G_\varphi(t_f)$ .  $\square$

**Lemma 5.2.** *Consider some values  $t_f > 0$  and  $\varphi \in [0, t_f)$ . Let  $S$  be a continuous closed curve without self-intersections in the plane  $x, y$ , and to any point of  $S$  at least one of the controls of the types U1, U2, U3, and U6 leads at the instant  $t_f$  (with the given value  $\varphi$ ). Suppose that the set  $S^-$  contains no points formed by controls of the types U1, U2, U3, and U6 for the mentioned values  $t_f$  and  $\varphi$ . Also assume that there is at least one point  $F \in S^-$  that does not belong to the set  $G_\varphi(t_f)$ . Then  $S \subset \partial G_\varphi(t_f)$  and  $G_\varphi(t_f) \cap S^- = \emptyset$ .*

The proof is similar to the proof of the previous lemma with the replacement of the set  $S^+$  by the set  $S^-$  and the point  $Q$  by the point  $F$ .

**Lemma 5.3.** *Consider some values  $t_f > 0$  and  $\varphi \in [0, t_f)$ . Let a set  $M$  in the plane of geometric coordinates  $x, y$  be open and connected. Assume that one of the following conditions is valid: 1) there are no points of curves A1, A2, A3, and A6 in the set  $M$ , but there is at least one point  $P \in \text{int}G_\varphi(t_f)$ ; 2) the set  $M$  contains some points of the curves A1, A2, A3, A6, and for all such points, except, perhaps, only one, it is known that they belong to the set  $\text{int}G_\varphi(t_f)$ . Then  $M \subset \text{int}G_\varphi(t_f)$ .*

*Proof.* Let condition 1) be satisfied. Suppose that the set  $M$  contains at least one point  $K \in \partial G_\varphi(t_f)$ . Taking into account Lemma 3.1, at least one of the controls of the type U1, U2, U3, and U6 leads to this point. But then the point  $K$  lies on one of the curves A1, A2, A3, and A6 that contradicts condition 1). Therefore,  $M \cap \partial G_\varphi(t_f) = \emptyset$ .

Suppose that in the set  $M$  there is some point  $L \notin G_\varphi(t_f)$ . Let us connect the points  $L$  and  $P$  by a continuous curve belonging to  $M$ . Then this curve will have at least one point from  $\partial G_\varphi(t_f)$  that is impossible.

Thus,  $M \subset \text{int}G_\varphi(t_f)$ .

Let condition 2) be satisfied. Denote by the symbol  $E$  the special point referred to in this condition. Consider the set  $V = M \setminus \{E\}$ . If the point  $E$  is missing, we consider  $V = M$ . The set  $V$  is open and connected. Repeating the reasoning scheme used in the first paragraph of the proof and taking into account the specifics of condition 2), we establish that  $V \cap \partial G_\varphi(t_f) = \emptyset$ .

From condition 2), taking into account the continuity of the curves A1, A2, A3, and A6, it follows that in the set  $V$  some point  $F \in \text{int}G_\varphi(t_f)$  exists. Suppose that there is a point  $L \notin G_\varphi(t_f)$  in the set  $V$ . We connect the points  $L$  and  $F$  by a continuous curve lying in  $V$ . Then this curve contains a point from  $\partial G_\varphi(t_f)$  that is impossible. Therefore,  $V \subset \text{int}G_\varphi(t_f)$ .

Since the open, connected sets  $V$  and  $M$  differ, perhaps, by only one point  $E$ , then  $M \subset \text{int}G_\varphi(t_f)$ .  $\square$



6. CLASSIFICATION OF  $\varphi$ -SECTIONS FOR  $\varphi \geq 0$ 

The shape of the  $\varphi$ -sections is determined by the values of  $\varphi$  and  $t_f$ . Assume that  $t_f > 0$  and  $\varphi \in [0, t_f]$ . We shall distinguish five sets in the space of values  $\varphi, t_f$ . Respectively, we consider five cases

$$\text{Case 1: } 0 \leq \varphi < t_f, \quad t_f < 4\pi - \varphi, \quad t_f < 3\pi + 2\cos(\varphi/2). \quad (6.1)$$

$$\text{Case 2: } 0 \leq \varphi < \pi, \quad t_f < 4\pi - \varphi, \quad t_f \geq 3\pi + 2\cos(\varphi/2). \quad (6.2)$$

$$\text{Case 3: } 0 \leq \varphi < 2\pi, \quad t_f \geq 4\pi - \varphi. \quad (6.3)$$

$$\text{Case 4: } 2\pi \leq \varphi < t_f. \quad (6.4)$$

$$\text{Case 5: } \varphi = t_f. \quad (6.5)$$

Let us establish that any point  $(\varphi, t_f)$  satisfying the conditions  $t_f > 0$  and  $0 \leq \varphi \leq t_f$  belongs to one and only one of the specified sets.

If  $\varphi = t_f$ , then the point  $(\varphi, t_f)$  belongs to Set 5 (Case 5). With that, it is obvious that the point  $(\varphi, t_f)$  does not come into Set 1 and Set 4. From the first and third conditions (6.2) in Case 2, it follows that  $t_f > 3\pi$ ; at the same time,  $\varphi < \pi$ . In Case 3, we have  $t_f > 2\pi$ . Thus, the point under consideration does not belong to Sets 1–4.

From the first two inequalities in (6.1), it follows that in Case 1 the inequality  $\varphi < 2\pi$  holds. Therefore, under condition (6.4), the point  $(\varphi, t_f)$  comes only into Set 4.

If  $0 \leq \varphi < \pi$ , then the inequality

$$4\pi - \varphi > 3\pi + 2\cos(\varphi/2) \quad (6.6)$$

holds. Indeed, the condition  $0 \leq \varphi < \pi$  can be rewritten as  $0 < (\pi - \varphi)/2 \leq \pi/2$ . Therefore, the inequality  $(\pi - \varphi)/2 > \sin((\pi - \varphi)/2)$  holds that is equivalent to (6.6). Inequality (6.6) means that for  $0 \leq \varphi < \pi$  in (6.1), the second condition follows from the third condition. Similarly, for  $\varphi \in [\pi, 2\pi)$ , we have

$$4\pi - \varphi \leq 3\pi + 2\cos(\varphi/2), \quad (6.7)$$

i.e., in (6.1), the third condition follows from the second one.

Let  $0 \leq \varphi < \pi$  and  $\varphi < t_f$ . Based on inequality (6.6), we establish that the point  $(\varphi, t_f)$  comes at  $t_f \in (\varphi, 3\pi + 2\cos(\varphi/2))$  only to Set 1; correspondingly, for  $t_f \in [3\pi + 2\cos(\varphi/2), 4\pi - \varphi)$ , it comes only to Set 2, and only to Set 3 for  $t_f \in [4\pi - \varphi, \infty)$ . Let  $\varphi \in [\pi, 2\pi)$  and  $\varphi < t_f$ . Using inequality (6.7), we get that the point  $(\varphi, t_f)$  belongs only to Set 1 for  $t_f < 4\pi - \varphi$  and only to Set 3 for  $t_f \geq 4\pi - \varphi$ .

Thus, the property of partition of the area  $\{(\varphi, t_f) : 0 \leq \varphi \leq t_f, t_f > 0\}$  into Sets 1–5 is established.

Sets 1–5 are shown in Fig. 11. For  $0 \leq \varphi < \pi$ , Set 1 is separated from Set 2 by the line  $t_f = 3\pi + 2\cos(\varphi/2)$  (the line is included into Set 2), and Set 2 is separated from Set 3 by a segment of the straight line  $t_f = 4\pi - \varphi$  (that is included into Set 3). For  $\pi \leq \varphi < 2\pi$ , Set 1 is separated from Set 3 by a segment of the straight line  $t_f = 4\pi - \varphi$ . This segment is included into Set 3. Set 3 is separated from Set 4 by an unlimited ray  $\varphi = 2\pi, t_f > \varphi$ . This ray is included into Set 4. Set 5 is an unlimited ray  $0 < \varphi = t_f$ .

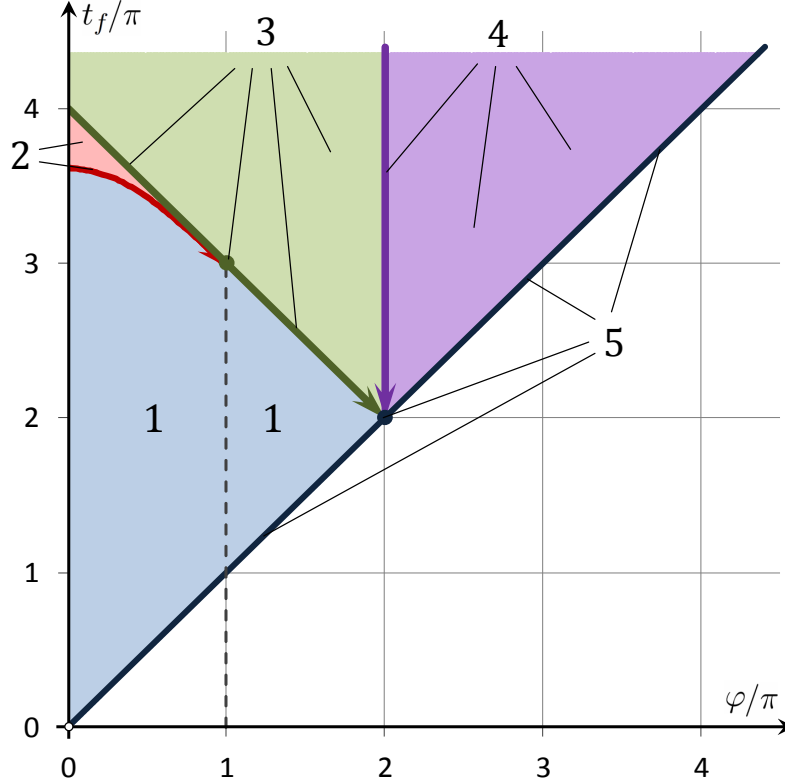


FIGURE 11. Classification of the  $\varphi$ -sections of the reachable set  $G(t_f)$  for values  $t_f > 0$  and  $0 \leq \varphi \leq t_f$

In Case 5, as noted in Section 3.1, any  $\varphi$ -section is a one-point set. Geometric coordinates in the original system are represented by the formulas  $x(t_f) = \sin t_f$  and  $y(t_f) = 1 - \cos t_f$ . Position of such a point in the auxiliary coordinate system has the form  $X(t_f) = 0, Y(t_f) = 0$ .

In the following Sections, we describe the  $\varphi$ -sections for Cases 1–4.

## 7. BOUNDARY OF $\varphi$ -SECTIONS FOR CASE 1

We assume that  $(\varphi, t_f)$  belongs to Set 1. The curves A1, A2, A3, and A6 are used as the basic elements of the boundary of the  $\varphi$ -sections. Each of them is fully included into the description of the boundary. This case is partially considered in [44] where it was assumed that  $t_f \leq 2\pi$ .

From the first two relations in (6.1), it follows that  $0 \leq \varphi < 2\pi$  and  $0 < \theta < 2\pi$  where  $\theta = (t_f - \varphi)/2$ . Considering formulas (3.10), (3.13) for the curves A1 and A6 (they are the arcs of circumferences), as well as the corresponding ranges of parameters  $s_1$  and  $s_3$  in (3.4), we conclude that in Case 1, the span of each of the arcs A1 and A6 is less than  $2\pi$ .

If  $\varphi = 0$ , then the arc A1 degenerates into a point coinciding with the starting point of the curve A3 and the end point of the curve A2. If  $\varphi > 0$ , the arc A1 is not degenerate. Its starting point is below the axis  $X$ , and its end point is above the axis  $X$ .

1) Let us show that the curves A2 and A3 in Case 1 have a common point only for  $\varphi = 0$ . Herewith, there is only one common point, which is their mutual joining point. It coincides with the degeneration point of the arc A1.

Investigate the curve A3. For the extreme values  $s_3 = 0$  and  $s_3 = \theta$ , we have

$$Y_{U_3}(0) = (t_f - \varphi) \sin\left(\frac{\varphi}{2}\right) \geq 0, \quad Y_{U_3}(\theta) = 4 \sin\left(\frac{t_f - \varphi}{4}\right) \sin\left(\frac{t_f + \varphi}{4}\right) > 0. \quad (7.1)$$

The first inequality follows from the fact that  $\varphi \in [0, 2\pi)$  and  $\varphi < t_f$ . Using the condition  $t_f < 4\pi - \varphi$ , we obtain the second inequality. The first inequality turns into the equality only for  $\varphi = 0$ .

Let us establish that  $Y_{U_3}(s_3) > 0$  for any  $s_3 \in (0, \theta)$ . We calculate the derivative of the function  $Y_{U_3}(s_3)$  with respect to  $s_3$ :

$$(Y_{U_3}(s_3))'_{s_3} = 2(\theta - s_3) \cos\left(s_3 + \frac{\varphi}{2}\right). \quad (7.2)$$

For  $s_3 \in (0, \theta)$ , the sign of the derivative is determined by the last factor, and the value  $s_3 + \varphi/2$  varies in the range  $(\varphi/2, t_f/2)$ . From the first two relations in (6.1), it follows that

$$0 \leq \varphi < t_f < 4\pi.$$

Therefore,  $(s_3 + \varphi/2) \in (0, 2\pi)$ . Within this extended range, the expression  $\cos(s_3 + \varphi/2)$  equals zero for only two values of the parameter  $s_3$ :  $s_3^* = (\pi - \varphi)/2$  and  $s_{3*} = (3\pi - \varphi)/2$ . These points do not always belong to the range  $(0, \theta)$  of admissible values  $s_3$ .

In Fig. 12, the curves A1, A2, A3, and A6 are shown for the same value  $\varphi = 0.5\pi$  and four values of  $t_f$ :  $0.99\pi$ ,  $2.3\pi$ ,  $2.8\pi$ ,  $3.3\pi$ . If  $t_f = 0.99\pi$ , then there are no values  $s_3^*$  and  $s_{3*}$  (defining horizontal tangents to the curve A3) in the interval  $(0, \theta)$ . If  $t_f = 2.3\pi$  or  $t_f = 2.8\pi$ , then  $s_3^* \in (0, \theta)$ ,  $s_{3*} \notin (0, \theta)$ . For  $t_f = 3.3\pi$ , we get  $s_3^* \in (0, \theta)$  and  $s_{3*} \in (0, \theta)$  (respectively, the curve A3 has two horizontal tangents).

Consider the value  $s_3^*$ . Due to (3.12), the value  $Y_{U_3}(s_3^*)$  is calculated by the formula

$$Y_{U_3}(s_3^*) = 2(\theta - s_3^*) \sin\left(s_3^* + \frac{\pi}{2}\right) + 4 \sin\frac{s_3^*}{2} \sin\left(\frac{s_3^*}{2} + \frac{\pi}{2}\right). \quad (7.3)$$

Condition  $s_3^* \in (0, \theta)$  can be written as  $0 < (\pi - \varphi)/2 < (t_f - \varphi)/2$ . It implies the fulfillment of the inequalities  $\varphi < \pi < t_f$ . Due to these inequalities, substituting the values of  $s_3^*$  and  $\theta$  into (7.3), we obtain

$$Y_{U_3}(s_3^*) = (t_f - \pi) + 4 \sin\left(\frac{\pi}{4} - \frac{\varphi}{4}\right) \sin\left(\frac{\pi}{4} + \frac{\varphi}{4}\right) > 0. \quad (7.4)$$

Consider the value  $s_{3*}$ . The condition  $s_{3*} \in (0, \theta)$  implies the inequality  $t_f > 3\pi$ . Taking into account the second relation in (6.1), we obtain the inequality  $\varphi < \pi$ . We calculate  $Y_{U_3}(s_{3*})$ :

$$Y_{U_3}(s_{3*}) = 3\pi - t_f + 4 \sin\left(\frac{3\pi}{4} - \frac{\varphi}{4}\right) \sin\left(\frac{3\pi}{4} + \frac{\varphi}{4}\right) = 3\pi - t_f + 2 \cos\left(\frac{\varphi}{2}\right). \quad (7.5)$$

Using the third relation in (6.1), we have

$$Y_{U_3}(s_{3*}) > 0. \quad (7.6)$$

We have inequalities (7.1) for the values of  $Y_{U_3}(s_3)$  at the extreme points of the curve A3 as well as inequalities (7.4), (7.6) for the interior points where the derivative  $(Y_{U_3}(s_3))'_{s_3}$  equals to zero. From it, we conclude that the curve A3 lies above the axis  $X$  (see two examples in Fig. 13) with the exception of the starting point at  $\varphi = 0$ .

Due to the symmetry of the curves A2 and A3 w.r.t. the axis  $X$ , the curve A2 lies below the axis  $X$  with the exception of the end point for  $\varphi = 0$ . Thus, the curves A2 and A3 for  $\varphi > 0$

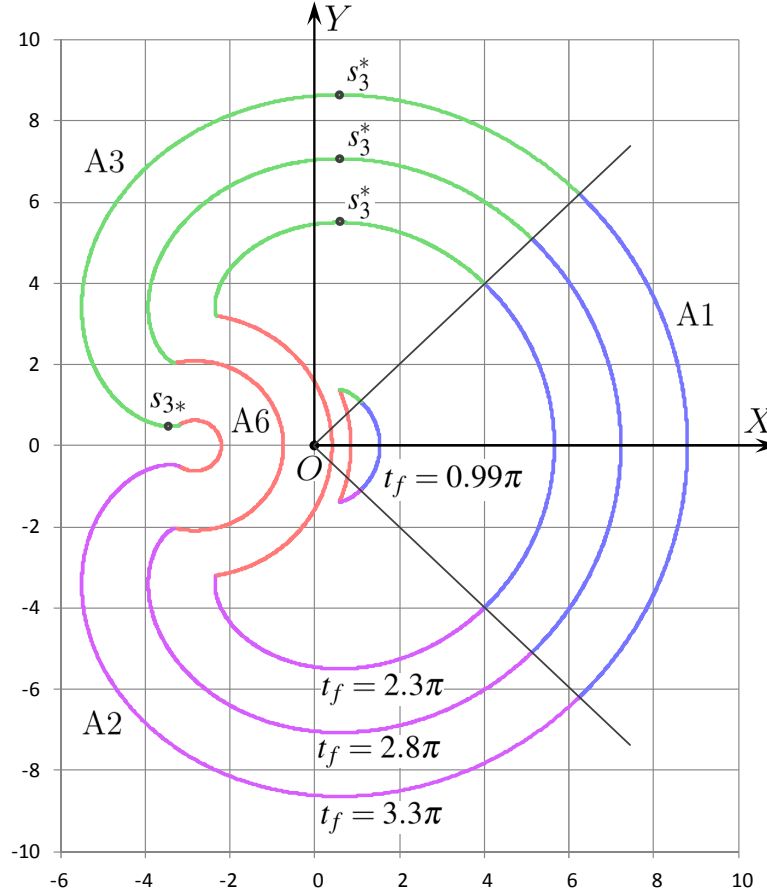


FIGURE 12. Glued curves  $A_\varphi(t_f)$  for the angle  $\varphi = 0.5\pi$  and four values  $t_f = 0.99\pi, 2.3\pi, 2.8\pi, 3.3\pi$ . Location of the points  $s_3^*, s_{3*}$  on the curves A3

have no common points, and for  $\varphi = 0$  the starting point of the curve A3 coincides with the end point of the curve A2.

2) In general, taking into account the results of Section 3, we see that the “glued” curve  $A_\varphi(t_f) = A1 \cup A3 \cup A6 \cup A2$  is a piecewise smooth closed one without self-intersections. The smoothness is broken only at the points of joining the arcs A2 and A3 with the arc A6 (Fig. 12). The glued curve contains *all* points of motion by the controls U1, U2, U3, and U6 for the given  $t_f$  and  $\varphi$ .

Let the symbol  $\mathbf{A}_\varphi(t_f)$  denote the closed set bounded by the curve  $A_\varphi(t_f)$ . By Lemma 5.1, this curve belongs to  $\partial G_\varphi(t_f)$  and the inclusion  $G_\varphi(t_f) \subset \mathbf{A}_\varphi(t_f)$  is true.

For  $\varphi \in (0, t_f)$ , consider the motion generated on the interval  $[0, t_f]$  by the constant control  $u(t) \equiv \varphi/t_f$ . Such the motion does not satisfy the PMP. Therefore, by virtue of [42], it leads to the  $\text{int}G_\varphi(t_f)$ , and, hence, to the  $\text{int}G_\varphi(t_f)$ . For  $\varphi = 0$ , as the similar motion (but with one switch), we take the motion with the control  $u(t) = -0.5$  for  $t \in [0, t_f/2)$  and  $u(t) = +0.5$  for  $t \in [t_f/2, t_f]$ . It also leads into  $\text{int}G_\varphi(t_f)$ . Turning to Lemma 5.3, we see that for the set  $M = \text{int}\mathbf{A}_\varphi(t_f)$  the condition 1) is satisfied. Therefore,  $\text{int}\mathbf{A}_\varphi(t_f) \subset G_\varphi(t_f)$ .

As a result, we get  $\mathbf{A}_\varphi(t_f) = G_\varphi(t_f)$ .

Two examples of the sets  $G_\varphi(t_f)$  for Case 1 are shown in Fig. 13. Scale of the image is determined by the radius of the circle  $C_{A1}$ .

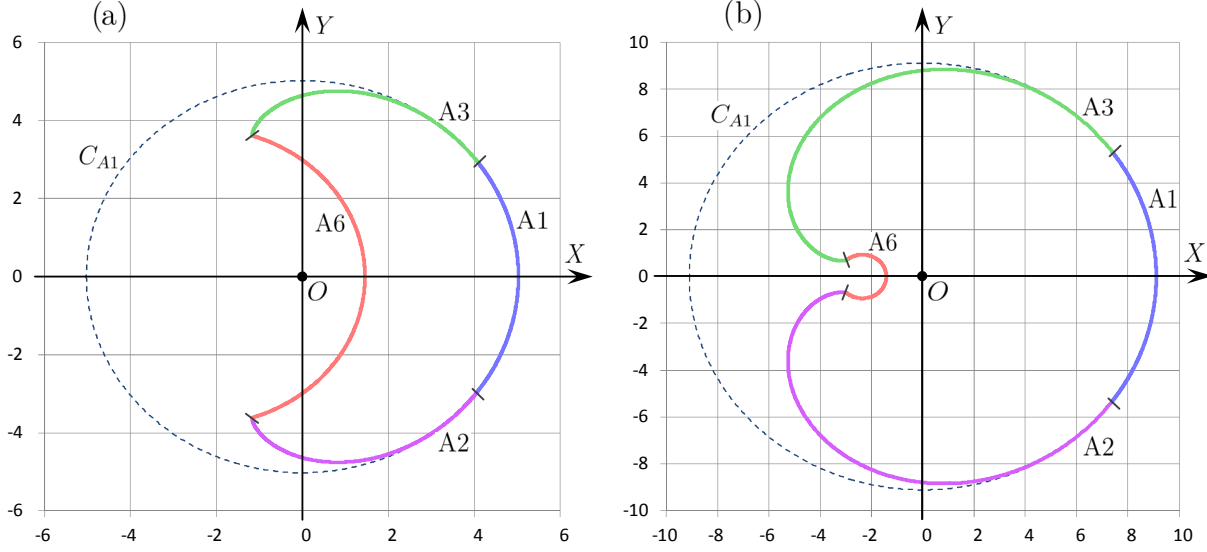


FIGURE 13. Variants of the sets  $G_\varphi(t_f)$  for Case 1 with  $\varphi = 0.4\pi$  and two values  $t_f = 2\pi$  (a) and  $t_f = 3.3\pi$  (b)

## 8. BOUNDARY OF $\varphi$ -SECTIONS FOR CASE 2

Let fix  $\varphi$  and  $t_f$  satisfying the conditions of Case 2. As in Case 1, the boundary of the  $\varphi$ -section will be constructed on the basis of the curves A1, A2, A3, and A6. The main feature is that any  $\varphi$ -section related to Case 2 is not simply connected.

**8.1. Points of intersection of the curves A2 and A3.** Each of the curves A2 and A3 is an involute arc. The curve A1 joins with the curves A2 and A3 with keeping of curvature continuity (Section 3.7, Property 7).

Based on (6.2), we prove that there are one or two points of intersection of the curves A2 and A3.

Consider the curve A3. For the extreme points (by analogy with Case 1 using the relations (7.1)), we obtain  $Y_{U3}(0) \geq 0$ ,  $Y_{U3}(\theta) > 0$ . The first inequality turns into the equality only for  $\varphi = 0$ .

For  $s_3 \in (0, \theta)$ , the derivative  $(Y_{U3}(s_3))'_{s_3}$  calculated by formula (7.2) becomes zero for values  $s_3^* = (\pi - \varphi)/2$  and  $s_{3*} = (3\pi - \varphi)/2$ . In Case 2 (unlike Case 1), these values always belong to the interval  $(0, \theta)$  due to (6.2). Therefore, the corresponding points on the curve A3 always exist.

As noted in Section 7, formula (7.4), we have  $Y_{U3}(s_3^*) > 0$  for the first point. For the second point, we get  $Y_{U3}(s_{3*}) = 3\pi - t_f + 2\cos(\varphi/2) \leq 0$  by virtue of (7.5) and the third inequality in (6.2).

Let

$$t_f > 3\pi + 2\cos(\varphi/2). \quad (8.1)$$

We show that under this condition, the curves A2 and A3 intersect at two points located on the negative part of the axis  $X$  (Fig. 14b). To do this, it is sufficient to consider the intersection points of the curve A3 with the axis  $X$  due to the symmetry of the curves A2 and A3 relatively to this axis.

Let us select three parts on the curve A3:  $s_3 \in (0, s_3^*)$ ,  $s_3 \in (s_3^*, s_{3*})$ , and  $s_3 \in (s_{3*}, \theta)$ . The function  $Y_{U3}(s_3)$  is strictly monotone on each of these parts. In the first part, there is no intersection with the axis  $X$ . On the second, there is one intersection point, let us designate it  $P_1$ . The third part also has one intersection point, we denote it by  $P_2$ . In general, we get two points of intersection of the curve A3 (with extreme points excluded) and the axis  $X$ . This property is also true for the curve A2. For  $\varphi = 0$ , in addition to the indicated points, the curves A2 and A3 are joined at the point of the curve A1 degeneration.

Let the equality

$$t_f = 3\pi + 2\cos(\varphi/2) \quad (8.2)$$

be fulfilled now. This equality corresponds to the situation when the curve A3 touches the axis  $X$  (and hence the curve A2) at the point  $(X_{U3}(s_{3*}), Y_{U3}(s_{3*}))^T$ . Herein, with the exception of the point of tangency, the interior points of the curve A3 lie above the axis  $X$ , and the interior points of the curve A2 are below the axis  $X$  (Fig. 14a). Thus, under condition (8.2) for  $\varphi > 0$ , the curves A2 and A3 have only one common point  $P_1 = P_2$  (this is the point of tangency defined on the curve A3 by the parameter  $s_3 = s_{3*}$ ). If  $\varphi = 0$ , then (as well as under condition (8.1)) the curves A2 and A3 are additionally joined at the point of degeneration of the curve A1.

### 8.2. Analysis of arcs of the curves A2 and A3 between the points of their intersection.

Consider under condition (8.1) an open arc of the curve A3 between the points  $P_1$  and  $P_2$  in the plane  $X, Y$ . This arc is located below the axis  $X$ . Let us show that it belongs to  $\text{int}G_\varphi(t_f)$ . We shall use Lemma 4.3. To ensure that the conditions of this Lemma are fulfilled, we establish that for any point  $P$  of this arc the corresponding motion (with a control of the type U3) has no cycles and each of three intervals of the control constancy is not degenerate.

For controls of the type U3, the switch instants  $t_1$  and  $t_2$  satisfy the relation  $\varphi = t_1 - (t_f - t_2)$ . The sum of the lengths of the first and third intervals does not exceed  $t_f$ . Therefore,  $2t_1 - \varphi = t_1 + (t_f - t_2) \leq t_f$ . For Case 2 (see (6.2)), the inequality  $t_f < 4\pi - \varphi$  holds. So,  $2t_1 - \varphi < 4\pi - \varphi$ , i.e.  $t_1 < 2\pi$ . It means that there are no cycles on the first interval. For  $\varphi \geq 0$ , the length of the third interval does not exceed the length of the first one. So, there are no cycles on the third interval also.

As noted in Section 3.7, Property 4, any control of the type U3 leading to an interior point  $P$  of the arc A3 has three non-degenerate intervals of constancy. Applying Lemma 4.3, we obtain  $(P, \varphi)^T \in \text{int}G(t_f)$ . Hence,  $P \in \text{int}G_\varphi(t_f)$ .

### 8.3. Description of the boundary of $\varphi$ -sections for Case 2 in the form of outer and inner contours.

The curve A6 is a circular arc. Its center (in the auxiliary coordinate system) is located at the point  $H$  by formula (3.15), and the radius  $R_{A6}$  is described by formula (3.16). From the second inequality in the definition of Case 2, it follows that the arc A6 is non-degenerate (the radius is not equal to zero).

The arc A6 (with parts of the curves A2 and A3 attached to it up to the second point  $P_2$  of their intersection) forms a closed curve. Let us denote it by  $B_\varphi(t_f)$ . The symbol  $A_\varphi(t_f)$  denotes the closed curve composed of the arc A1 with parts of the curves A2 and A3 attached to it at the

first point  $P_1$  of their intersection (see Fig. 14). When  $\varphi = 0$ , the arc A1 degenerates into a point that becomes the junction point of the curves A2 and A3. Therefore, for  $\varphi = 0$ , we can assume that the closed curve  $\mathbf{A}_\varphi(t_f)$  is formed by two curves A2 and A3 (up to the point  $P_1$ ). Each of the curves  $\mathbf{A}_\varphi(t_f)$  and  $\mathbf{B}_\varphi(t_f)$  has no self-intersections. Let  $\mathbf{A}_\varphi(t_f)$  (respectively,  $\mathbf{B}_\varphi(t_f)$ ) be a closed set bounded by the curve  $\mathbf{A}_\varphi(t_f)$  (respectively, curve  $\mathbf{B}_\varphi(t_f)$ ).

The examples of the sets  $\mathbf{A}_\varphi(t_f)$  and  $\mathbf{B}_\varphi(t_f)$  are shown in Fig. 14.

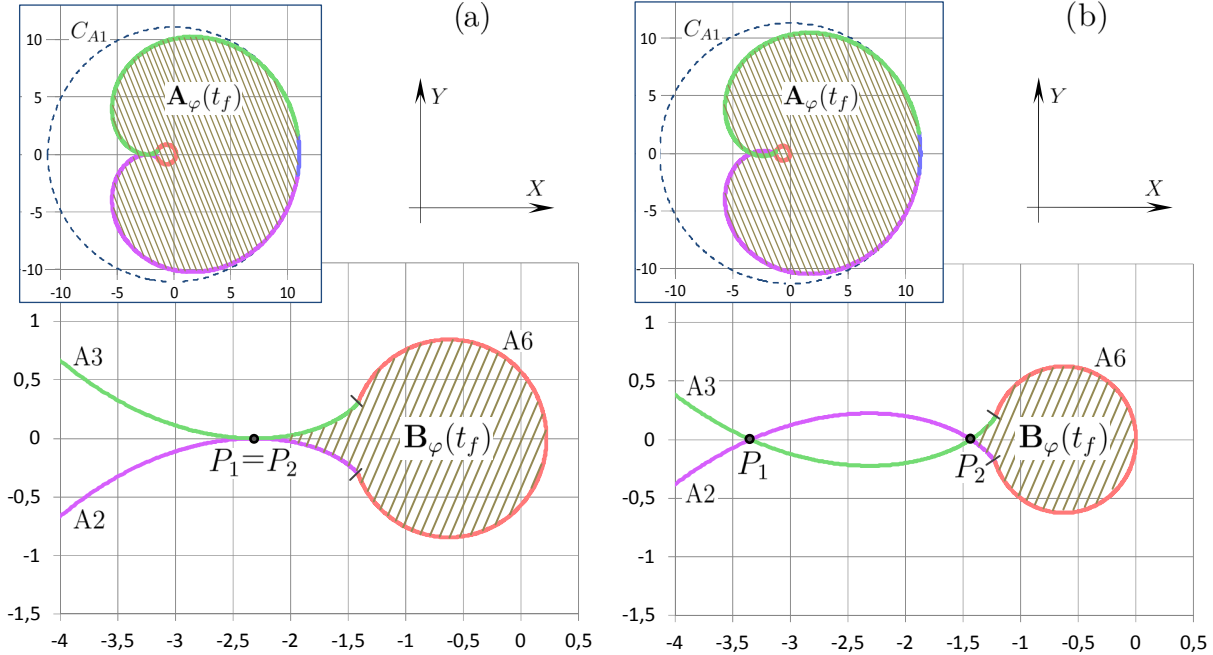


FIGURE 14. The sets  $\mathbf{A}_\varphi(t_f)$  and  $\mathbf{B}_\varphi(t_f)$  for Case 2 with  $\varphi = 0.1\pi$  and two values  $t_f = 3\pi + 2\cos(0.05\pi)$  (a) and  $t_f = 3.7\pi$  (b)

When fulfilling inequality (8.1), the arcs of the curves A2 and A3 between the points  $P_1$  and  $P_2$  of their intersection lie in the  $\text{int}G_\varphi(t_f)$ .

1) Consider two circles centered at the point  $H$ : one passes through the point  $P_1$ , the other goes through the point  $P_2$ . The corresponding circles will be denoted by  $C_{P_1}$  and  $C_{P_2}$ . In Section 3.7 (Properties 5 and 6), it was noted that, for the parametrically defined curves A2 and A3, there is the monotonic change of the distance from the point  $H$  to the points of the curves A2 and A3. From this, it follows that the circle  $C_{A_6}$  (with the center  $H$ ), on the boundary of which the curve A6 lies, belongs to the set  $\mathbf{B}_\varphi(t_f)$ . Besides, for (8.1), the circle  $C_{P_1}$  covers the circle  $C_{P_2}$ , and for (8.2), these circles coincide.

Additionally, taking into account Property 10 of Section 3.7, we get that the curve  $\mathbf{A}_\varphi(t_f)$  (excepting the point  $P_1$ ) lies outside the circle  $C_{P_1}$ . The remaining parts of the curves A2, A3, and, also, the curve A6 are located in the  $\text{int}C_{P_1}$ . Similarly, the curve  $\mathbf{B}_\varphi(t_f)$  (excepting the point  $P_2$ ) lies in the  $\text{int}C_{P_2}$ ; the remaining parts of the curves A2, A3, and the whole curve A1 are outside the circle  $C_{P_2}$ .



Outside the set  $\mathbf{A}_\varphi(t_f)$ , there are no points generated by controls of the types U1, U2, U3, and U6. Therefore, by virtue of Lemma 5.1, the curve  $A_\varphi(t_f)$  forms the “outer” boundary of the set  $G_\varphi(t_f)$  for Case 2.

2) Now, let us establish that the curve  $\mathbf{B}_\varphi(t_f)$  is the “inner” boundary of the set  $G_\varphi(t_f)$ .

2.1) Consider in the set  $\text{int}\mathbf{B}_\varphi(t_f)$  a point  $J$  located on the axis  $X$  and spaced from the point  $H$  to the left by  $\frac{1}{2}R_{A6}(t_f)$ . We have

$$J = \left( -4 \sin\left(\frac{\varphi}{2}\right) - 2 \sin\left(\frac{t_f + \varphi}{4}\right), 0 \right)^\top.$$

We shall show that  $J \notin G_\varphi(t_f)$ . Suppose the opposite, i.e.,  $J \in G_\varphi(t_f)$ . Then by Filippov’s theorem [50], there is an *time-optimal* control leading to the phase point  $(J, \varphi)^\top$ . Let  $t_f^*$  be the corresponding time-optimal instant. We have  $0 \leq t_f^* \leq t_f$ .

By virtue of Theorem 1 of [1, p. 515], the time-optimal control can be taken in the form of one of six variants U1 – U6. Let us consider them. At the same time, for the U5 and U6 control types, we do not suppose obligatory to fulfill condition (3.2).

Any control of the type U4 gives the value  $\varphi \leq 0$  at the instant  $t_f^*$ . Since we assume  $0 \leq \varphi < \pi$  (see. (6.2)), then for U4 we have to consider only the value  $\varphi = 0$  with the control  $u(\cdot) \equiv 0$ . Here, we get the point  $(x(t_f^*), y(t_f^*))^\top = (t_f^*, 0)^\top$ . It does not coincide with the point  $J$  for any  $t_f^* \in [0, t_f]$ .

To provide the inequality  $\varphi > 0$  at the instant  $t_f^*$  with a control of the type U5, it is required that the length of the middle interval of the control constancy to be less than the sum of the lengths of the first and third intervals. In paper [40] (the proof of Lemma 2) for such a condition, it was established that there is another motion that comes exactly to the same phase point at the same instant  $t_f^*$ , but it does not satisfy the PMP. So, the instant  $t_f^*$  is not time-optimal. Thus, any controls of the type U5 cannot be time-optimal to arrive to the point  $(J, \varphi)^\top$  for  $\varphi > 0$ .

If  $\varphi = 0$ , then controls of the type U5 generate the same set of points  $(x, y)$  at the instant  $t_f^*$  as controls of the type U6. Therefore, controls of the type U5 need not be considered.

Controls of four types remain: U1, U2, U3, and U6. Let us introduce the notations  $A1^*$ ,  $A2^*$ ,  $A3^*$ , and  $A6^*$  for the curves generated by the indicated controls at the time-optimal instant  $t_f^* \in [\varphi, t_f]$  with the fixed value  $\varphi$ . These curves are calculated using formulas (3.10)–(3.13) and (3.4) with the  $t_f$  symbol replaced by  $t_f^*$  one. Let us show that the curves  $A1^*$ ,  $A2^*$ ,  $A3^*$ , and  $A6^*$  do not contain the point  $J$ .

Consider two variants:  $t_f^* \in [\varphi, \pi)$ ,  $t_f^* \in [\pi, t_f]$ .

In the first variant, you can make sure that the curves  $A1^*$ ,  $A2^*$ ,  $A3^*$ , and  $A6^*$  are located in the half-plane  $X \geq 0$ . At the same time, the point  $J$  is in the half-plane  $X < 0$ . Therefore, any controls of the types U1, U2, U3, and U6 cannot be the solution of the time-optimal problem for  $t_f^*$ .

In the second variant, the inequality  $\pi/4 \leq (t_f^* + \varphi)/4$  is true. We show that  $J \in \text{int}C_{A6^*}$ . To do this, it is enough to establish that the distance  $2 \sin((t_f^* + \varphi)/4)$  between the points  $J$  and  $H$  is less than the radius  $R_{A6}(t_f^*) = 4 \sin((t_f^* + \varphi)/4)$  of the circumference corresponding to the arc  $A6^*$  (see (3.16)). The modulus sign in the formula for  $R_{A6}(t_f^*)$  is omitted, since (by virtue of  $0 \leq t_f^* + \varphi \leq t_f + \varphi < 4\pi$ ) the inequality  $\sin((t_f^* + \varphi)/4) \geq 0$  is fulfilled.

So, let us check the inequality

$$2 \sin((t_f + \varphi)/4) < 4 \sin((t_f^* + \varphi)/4). \quad (8.3)$$

If  $(t_f^* + \varphi)/4 \geq \pi/2$ , then inequality (8.3) is satisfied due to the monotonicity of the sine for the values  $\pi/2 \leq (t_f^* + \varphi)/4 \leq (t_f + \varphi)/4 < \pi$ . The last inequality follows from the definition of Case 2. If  $(t_f^* + \varphi)/4 < \pi/2$ , then  $4 \sin((t_f^* + \varphi)/4) \geq 4 \sin(\pi/4) = 2\sqrt{2}$ . From here, taking into account  $2 \sin((t_f + \varphi)/4) \leq 2$ , inequality (8.3) follows.

Since the arc  $A6^*$  lies on the boundary of the circle  $C_{A6^*}$ , any control of the type U6 cannot lead to the phase point  $(J, \varphi)^\top$  at the instant  $t_f^*$ .

From Section 3.7, Property 9, it follows that the curves  $A1^*$ ,  $A2^*$ , and  $A3^*$  are located outside the  $\text{int}C_{A6^*}$ . Therefore, controls of the types U1, U2, and U3, also, cannot lead to the phase point  $(J, \varphi)^\top$  at the instant  $t_f^*$ .

Thus, none of controls of the types U1–U6 can give solutions to the time-optimal problem to the point  $(J, \varphi)^\top$  at the instant  $t_f^*$ . Therefore, the instant  $t_f^* \in [0, t_f]$  cannot be the time-optimal one. We came to a contradiction. Therefore,  $J \notin G_\varphi(t_f)$ .

2.2) As noted above, the curve  $B_\varphi(t_f)$  (excepting the point  $P_2$ ) is located in the  $\text{int}C_{P2}$ . Besides the curve  $B_\varphi(t_f)$ , there are no other points in this circle formed by controls of the types U1, U2, U3, and U6. So, in the set  $\text{int}B_\varphi(t_f)$ , there are no points generated by these controls for the considered values  $t_f$  and  $\varphi$ .

Using Lemma 5.2, we see that all its conditions are fulfilled. As a result, we get that the curve  $B_\varphi(t_f)$  forms the “inner” boundary of the  $\varphi$ -section of the set  $G(t_f)$  for Case 2.

Consider the open set  $M_\varphi(t_f) = (A_\varphi(t_f))^- \cap (B_\varphi(t_f))^+$ . The curves  $A_\varphi(t_f)$  and  $B_\varphi(t_f)$  have at most one common point. Such a point is one of tangency of the curves  $A2$  and  $A3$  under condition (8.2). If this condition is not true, then the curves  $A_\varphi(t_f)$  and  $B_\varphi(t_f)$  have not the common points. Based on the Jordan and Schoenflies theorems [48, 49], it can be shown that the set  $M_\varphi(t_f)$  is connected.

Thus, the conditions of Lemma 5.3 are satisfied for the set  $M = M_\varphi(t_f)$ . We conclude that the set  $G_\varphi(t_f)$  in Case 2 has the external boundary in the form of the curve  $A_\varphi(t_f)$  and the inner boundary in the form of the curve  $B_\varphi(t_f)$ . We have  $G_\varphi(t_f) = A_\varphi(t_f) \setminus \text{int}B_\varphi(t_f)$  (Fig. 14).

## 9. BOUNDARY OF $\varphi$ -SECTIONS FOR CASE 3

The peculiarity of Case 3 is that the curve  $A6$  will not be used in the description of the boundary of the  $\varphi$ -sections. To construct the boundary, some partition of the curves  $A2$  and  $A3$  will be required.

**9.1. Partition of the curves  $A2$  and  $A3$ .** The required partition of the curve  $A3$  is described below in three subpoints. Due to the symmetry about the axis  $X$ , the similar partition takes place for the curve  $A2$ .

1) The curve  $A3$  is defined by formula (3.12) and given with the help of the parameter  $s_3 \in [0, \theta]$ . Let us put  $s_3^c = 2\pi - \varphi$ . Now, we show that  $s_3^c \in (0, \theta]$ . Indeed, it follows from the inequality  $\varphi < 2\pi$  in the definition of Case 3 that  $s_3^c > 0$ . The second relation in the definition of Case 3 is written as  $t_f - \varphi \geq 4\pi - 2\varphi$ . Therefore,  $s_3^c \leq (t_f - \varphi)/2 = \theta$ . Thus, the value  $s_3 = s_3^c$  defines some point on the curve  $A3$ , which we denote as  $\mathcal{P}_3^c$ . The point  $\mathcal{P}_3^c$  does not coincide with the starting point of the curve  $A3$ , but it may coincide with the curve last point.

Meaningfully, the parameter  $s_3^c$  corresponds to the value  $t_1 = 2\pi$  (by virtue of (3.3)). Therefore, there is a cycle on the first constancy interval of the arising control of the type U3. For  $s_3 < s_3^c$ , the corresponding motion does not contain cycles. For  $s_3 > s_3^c$ , the duration  $t_1$  of the first interval satisfies the relation  $t_1 > 2\pi$ . Thus, there is at least one cycle on the first interval.

Figure 15 shows the example of the curve A3 corresponding to  $t_f = 3.5\pi$ ,  $\varphi = 1.2\pi$ . Here,  $\theta = 1.15\pi$ . Dashed trajectories are constructed for five values of the parameter  $s_3$ . The trajectory leading to the point  $\mathcal{P}_3^c$  corresponds to the value  $s_3^c = 0.8\pi$ . For  $s_3 \in [0, 0.8\pi)$ , the first interval of the control constancy has the duration less than  $2\pi$ . Therefore, there are no cycles on the corresponding trajectories. For  $s_3 \in [0.8\pi, 1.15\pi]$ , there is a cycle on the first interval and there is no cycle on the third interval.

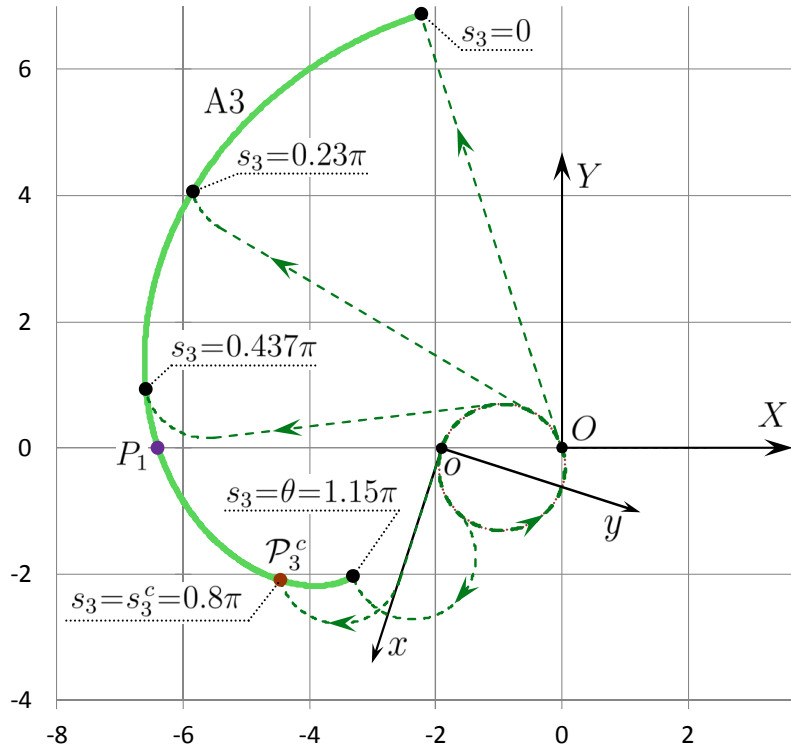


FIGURE 15. Example of the point  $\mathcal{P}_3^c$  location on the curve A3 ( $t_f = 3.5\pi$  and  $\varphi = 1.2\pi$ )

There may be cycles on the third interval of the control constancy, but then there should be also a cycle on the first interval, since  $\varphi = t_1 - (t_f - t_2) \geq 0$ .

The corresponding example of the curve A3 for  $t_f = 7.2\pi$ ,  $\varphi = 1.2\pi$  is shown in Fig. 16. Dashed trajectories are constructed for seven values of the parameter  $s_3$ . Among them, there is a trajectory leading to the point  $\mathcal{P}_3^c$ . Since the taken value of  $\varphi$  is the same as for Fig. 15, then the values  $s_3^c = 2\pi - \varphi$  are also the same. If  $s_3 \in [0, 0.8\pi)$ , then there are no cycles on the corresponding motion. For  $s_3 \in [0.8\pi, 2\pi)$ , there is only one cycle and it is located in the first interval. If  $s_3 = 2\pi$ , then the additional cycle arises on the third interval. For  $s_3 > 2\pi$ , there are cycles in both the first and third intervals.

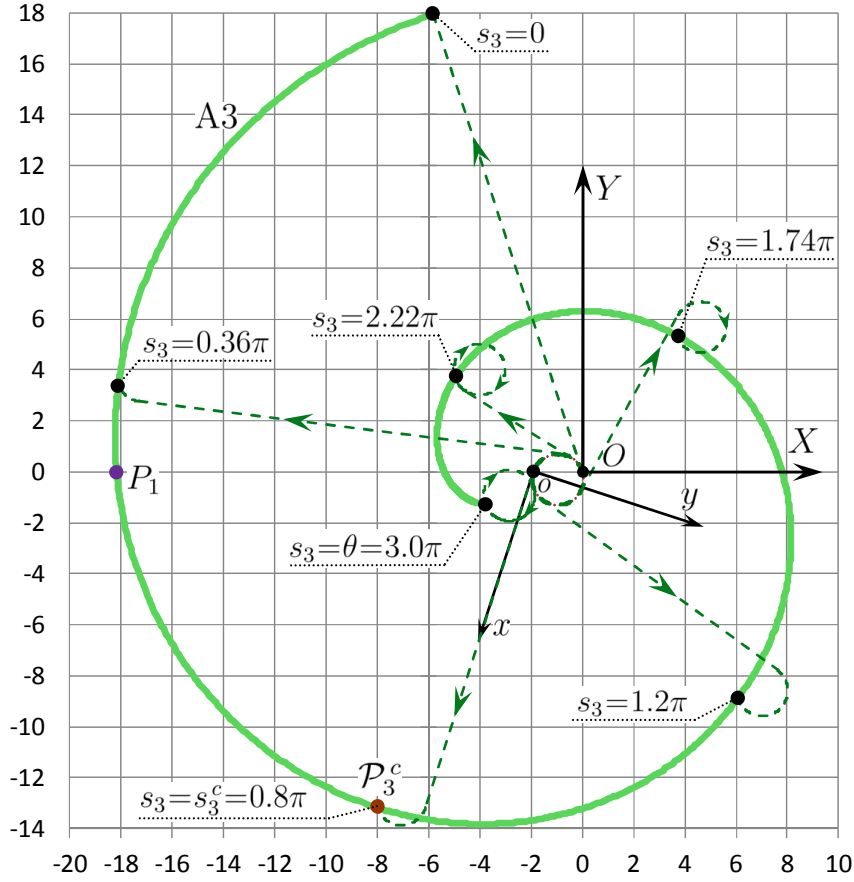


FIGURE 16. Example of the curve A3 with cycles on the first and third intervals of its generating trajectories ( $t_f = 7.2\pi$  and  $\varphi = 1.2\pi$ )

The point  $\mathcal{P}_3^c$  cannot lie above the axis  $X$ , i.e.,  $Y_{U3}(s_3^c) \leq 0$ . Indeed, let us substitute  $s_3^c = 2\pi - \varphi$  in (3.12). For the coordinate  $Y$  of the resulting point on curve A3, we have

$$Y_{U3}(s_3^c) = 2 \left( (\theta - 2\pi + \varphi) \sin \left( 2\pi - \varphi + \frac{\varphi}{2} \right) + 2 \sin \left( \pi - \frac{\varphi}{2} \right) \sin \left( \pi - \frac{\varphi}{2} + \frac{\varphi}{2} \right) \right).$$

Revealing the value  $\theta$  after simplifications, we get

$$Y_{U3}(s_3^c) = 2 \left( \frac{\varphi - t_f}{2} + 2\pi - \varphi \right) \sin \left( \frac{\varphi}{2} \right) = (4\pi - \varphi - t_f) \sin \left( \frac{\varphi}{2} \right).$$

It follows from the second relation in the definition of Case 3 that the first factor of the last expression is not positive. The second factor is not negative because  $0 \leq \varphi < 2\pi$ . Therefore,  $Y_{U3}(s_3^c) \leq 0$ . The equality  $Y_{U3}(s_3^c) = 0$  is equivalent to fulfillment of at least one of the conditions  $\varphi = 0, t_f = 4\pi - \varphi$ .

2) From the definition of Case 3, it follows that  $t_f \geq 2\pi$ . Thus, in Case 3, the relations  $0 \leq \varphi < 2\pi, \varphi < t_f$  hold. Therefore, the first inequality from (7.1) (established for Case 1) is valid. This means that the starting point  $\mathcal{P}_{1,3}$  of the curve A3 is above the axis  $X$  (for  $\varphi > 0$ ), or on this axis (for  $\varphi = 0$ ).

Consider a part of the curve A3 from the starting point  $\mathcal{P}_{1,3}$  to the point  $\mathcal{P}_3^c$ . We shall show that on this part there is a point  $P_1$  lying on the axis  $X$  such that the open arc  $(\mathcal{P}_{1,3}, P_1)$  is located

above the axis  $X$ , and then, the open arc  $(P_1, \mathcal{P}_3^c)$  is below the axis  $X$ . The point  $P_1$  can coincide with the point  $\mathcal{P}_3^c$ .

To establish existence of the point  $P_1$  (by analogy with Case 2), we investigate the derivative  $(Y_{U3}(s_3))'_{s_3}$ , which is calculated by formula (7.2). Let us consider the function  $s_3 \rightarrow (Y_{U3}(s_3))'_{s_3}$  on the interval  $(0, s_3^c)$ , which corresponds to the arc  $(\mathcal{P}_{1,3}, \mathcal{P}_3^c)$ .

If  $\varphi \geq \pi$ , we get  $(Y_{U3}(s_3))'_{s_3} < 0$  for  $s_3 \in (0, s_3^c)$ . We have  $Y_{U3}(0) > 0$  and  $Y_{U3}(s_3^c) \leq 0$ . Therefore, it is possible to uniquely determine the point  $P_1$  of intersection of the arc  $(\mathcal{P}_{1,3}, \mathcal{P}_3^c]$  with the axis  $X$ .

For  $\varphi < \pi$ , the function  $s_3 \rightarrow (Y_{U3}(s_3))'_{s_3}$  (as in Case 2) on the interval  $(0, s_3^c)$  vanishes only at two points  $s_3^* = (\pi - \varphi)/2$  and  $s_{3*} = (3\pi - \varphi)/2$ . It is not difficult to establish that  $0 < s_3^* < s_{3*} < s_3^c$ . We have  $(Y_{U3}(s_3))'_{s_3} > 0$  on the interval  $(0, s_3^*)$ . Therefore,  $Y_{U3}(s_3^*) > 0$ . Similarly, we have  $(Y_{U3}(s_3))'_{s_3} > 0$  on the interval  $(s_{3*}, s_3^c)$  that means  $Y_{U3}(s_{3*}) < 0$ . In turn, on the interval  $(s_3^*, s_{3*})$ , the derivative satisfies the relation  $(Y_{U3}(s_3))'_{s_3} < 0$ . Therefore, on this part of the curve A3 (as well as for  $\varphi \geq \pi$ ), it is possible to uniquely define the point  $P_1$  of intersection with the axis  $X$ .

Thus, on the arc  $(\mathcal{P}_{1,3}, \mathcal{P}_3^c]$  of the curve A3, you can specify the point  $P_1$  on the  $X$  axis so that the arc  $(\mathcal{P}_{1,3}, P_1)$  of the curve A3 lies above the axis  $X$ . With that, the remaining part  $(P_1, \mathcal{P}_3^c)$  of the curve A3 (if  $P_1 \neq \mathcal{P}_3^c$ ) is located below the axis  $X$ . It can be done both for  $\varphi \geq \pi$  and for  $\varphi < \pi$ .

3) If the point  $\mathcal{P}_3^c$  does not coincide with the point  $P_1$ , then consider an open arc  $(P_1, \mathcal{P}_3^c)$  of the curve A3 (see Figs. 15 and 16). For any point  $P$  of this arc, the control of the type U3 leading to it has three non-degenerate intervals of control constancy (see Section 3.7, Property 4). The corresponding trajectory has no cycles by definition of the point  $\mathcal{P}_3^c$ . The arc  $(P_1, \mathcal{P}_3^c)$  lies below the axis  $X$ . By Lemma 4.3, we see that the point  $(P, \varphi)^\top$  belongs to the  $\text{int}G(t_f)$ .

**9.2. Non-degenerate and degenerate subcases.** We shall distinguish two subcases of Case 3:

$$t_f > 4\pi - \varphi, \quad (9.1)$$

$$t_f = 4\pi - \varphi. \quad (9.2)$$

The first one will be called non-degenerate, the second one is degenerate.

1) Non-degenerate subcase. Rewrite condition (9.1) as  $t_f - \varphi > 4\pi - 2\varphi$ . Then, it follows that the point  $\mathcal{P}_3^c$  defined by the parameter  $s_3^c = 2\pi - \varphi$  does not coincide with the point  $\mathcal{P}_{3,6}$  corresponding to the parameter  $s_3 = \theta$ . Consider the half-open arc  $[\mathcal{P}_3^c, \mathcal{P}_{3,6})$  of the curve A3. For any point  $P$  of this arc, the respective control of the type U3 leading to this point has three non-degenerate intervals of control constancy. Moreover, the first interval contains a cycle due to the choice of the point  $\mathcal{P}_3^c$ . By Lemma 4.1, we obtain that  $(P, \varphi)^\top \in \text{int}G(t_f)$ .

Thus, the arc  $(P_1, \mathcal{P}_3^c) \cup [\mathcal{P}_3^c, \mathcal{P}_{3,6})$  is located in the  $\text{int}G_\varphi(t_f)$ .

The last point  $\mathcal{P}_{3,6}$  of the curve A3 is simultaneously the extreme point of the curve A6.

Consider the curve A6. Take an arbitrary point  $P$  on it. For the switch instants  $t_1$  and  $t_2$  of the control of the type U3 (which leads to this point), the following relations hold:

$$t_f = (t_1 - t_0) + (t_2 - t_1) + (t_f - t_2), \quad \varphi = -(t_1 - t_0) + (t_2 - t_1) - (t_f - t_2).$$

Substituting these expressions into the inequality  $t_f > 4\pi - \varphi$ , we get  $(t_2 - t_1) > 2\pi$ . Therefore, the length of the middle interval of the control U6 constancy is greater than  $2\pi$ . From the

condition  $\varphi < t_f$  satisfied to Case 3 (see (6.3)), it follows that the first and third intervals of control constancy cannot simultaneously degenerate.

Using Lemma 4.2, we obtain  $(P, \varphi)^\top \in \text{int}G(t_f)$ . Therefore,  $P \in \text{int}G_\varphi(t_f)$ . Thus, the whole curve A6 belongs to the  $\text{int}G_\varphi(t_f)$ .

For subcase (9.1), we get the following result. The curve A1 together with the part of the curve A3 (from the point  $\mathcal{P}_{1,3}$  to the point  $P_1$ ) and the part of the curve A2 (from the point  $P_1$  to the point  $\mathcal{P}_{1,2}$ ) form a closed curve without self-intersections. Denote it as  $\mathbf{A}_\varphi(t_f)$ . Let  $\mathbf{A}_\varphi(t_f)$  be the closed set bounded by this curve. The curve A6 and the remaining parts of the curves A2 and A3 belong to the set  $\text{int}\mathbf{A}_\varphi(t_f)$ , and they are also in the  $\text{int}G_\varphi(t_f)$ .

Figure 4b in Section 3 refers to Case 3, the non-degenerate subcase. It can be seen that the curve A3 after the first crossing the axis  $X$  (point  $P_1$ ) makes several revolutions. The part of this curve after the point  $P_1$  lies in the  $\text{int}G_\varphi(t_f)$ . Similarly, the same fact takes place for the part of the curve A2 symmetric to A3.

2) Degenerate subcase. From condition (9.2) and by analogy with the non-degenerate subcase, it follows that  $\mathcal{P}_3^c = \mathcal{P}_{3,6}$ . Here, the curve A6 degenerates (the radius of the circle becomes equal to zero) into the point  $H = \mathcal{P}_{2,6} = \mathcal{P}_{3,6}$ . If  $\varphi = 0$ , then the curve A1 degenerates into the point coinciding with the points  $\mathcal{P}_{1,2}$  and  $\mathcal{P}_{1,3}$ .

For the degenerate subcase in Fig. 17, the curve  $\mathbf{A}_\varphi(t_f)$  composed of the curves A1, A3, A6 (degenerate one), and A2 is shown. The point  $\mathcal{P}_3^c$  coincides with the point  $H$ . Three variants are presented here:  $\varphi = 0.3\pi$ ,  $t_f = 3.7\pi$  (Fig. 17a);  $\varphi = 1.0\pi$ ,  $t_f = 3.0\pi$  (Fig. 17b);  $\varphi = 1.4\pi$ ,  $t_f = 2.6\pi$  (Fig. 17c).

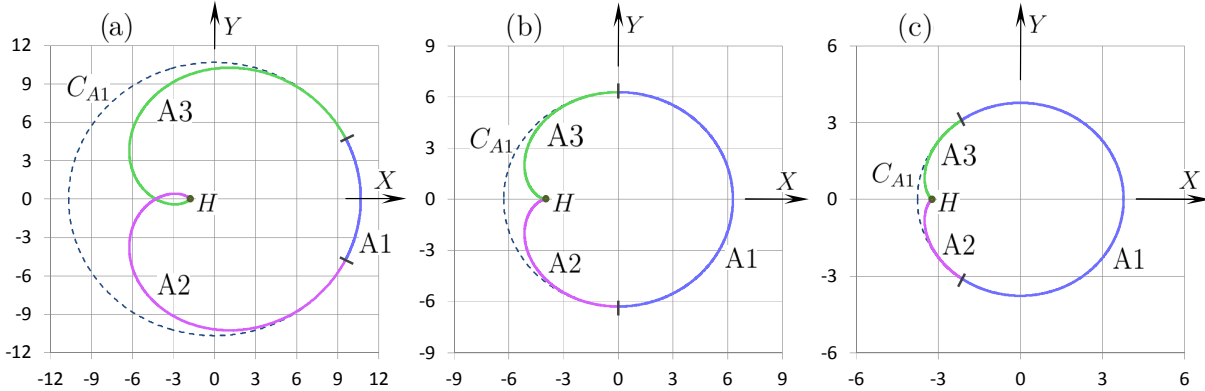


FIGURE 17. Case 3. Variants of the curve  $\mathbf{A}_\varphi(t_f)$  for the degenerate subcase

2.1) Suppose that  $\varphi < \pi$  (Fig. 17a). Then  $P_1 \neq \mathcal{P}_{3,6}$ . As in the non-degenerate subcase, the curve A1 together with a part of the curve A3 (from the point  $\mathcal{P}_{1,3}$  to the point  $P_1$ ) and a part of the curve A2 (from the point  $P_1$  to the point  $\mathcal{P}_{1,2}$ ) form the closed curve without self-intersections. Let  $\mathbf{A}_\varphi(t_f)$  be the closed set bounded by this curve. Under this, the arc  $(\mathcal{P}_{2,6}, P_1)$  of the curve A2 and the arc  $(P_1, \mathcal{P}_{3,6})$  of the curve A3 are in the  $\text{int}G_\varphi(t_f)$ . The similar property for the point  $\mathcal{P}_{2,6} = \mathcal{P}_{3,6}$  will be established in the next subsection.

2.2) Suppose  $\varphi \geq \pi$ . Then,  $P_1 = \mathcal{P}_{3,6}$ . We get that the curves A1, A2, and A3 form the closed curve without self-intersections. Let  $\mathbf{A}_\varphi(t_f)$  be the closed set bounded by this curve.



Geometrically, the situations  $\varphi = \pi$  (Fig. 17b) and  $\varphi > \pi$  (Fig. 17c) differ: in the first of them, the curves A2 and A3 touch at the point  $H = P_1$ , and in the second situation, they join at this point at some angle.

Outside the set  $\mathbf{A}_\varphi(t_f)$ , as well as in its interior, there are no points generated by controls of the types U1, U2, U3, and U6.

**9.3. Constructing the boundary of  $\varphi$ -section.** Applying Lemma 5.1 to the set  $\mathbf{A}_\varphi(t_f)$  introduced in the previous Section 9.2, we obtain that

$$G_\varphi(t_f) \subset \mathbf{A}_\varphi(t_f), \quad \partial \mathbf{A}_\varphi(t_f) \subset \partial G_\varphi(t_f). \quad (9.3)$$

Let us show that for the set  $\text{int} \mathbf{A}_\varphi(t_f)$  the conditions of Lemma 5.3 are satisfied. We put  $M_\varphi(t_f) = \text{int} \mathbf{A}_\varphi(t_f)$ .

In the non-degenerate subcase, all arcs of the curves A2, A3, and A6 that do not participate in formation of boundary of the set  $\mathbf{A}_\varphi(t_f)$  belong to the set  $M_\varphi(t_f)$ . Moreover, these arcs belong to the  $\text{int} G_\varphi(t_f)$ . Therefore, condition 2) of Lemma 5.3 is satisfied for the set  $M = M_\varphi(t_f)$ .

In the degenerate subcase for  $\varphi < \pi$ , condition 2) of Lemma 5.3 is satisfied. Indeed, for the parts of the curves A2, A3, and A6 that belong to the set  $M_\varphi(t_f)$ , it has been established that any point of them (excepting, perhaps, only the point  $\mathcal{P}_{3,6}$ ) belongs to the  $\text{int} G_\varphi(t_f)$ . For  $\varphi \geq \pi$  there are no the curves A1, A2, A3 and A6 outside the set  $\partial \mathbf{A}_\varphi(t_f)$ , and, therefore, these curves are absent in the set  $M_\varphi(t_f)$ . To apply Lemma 5.3 (under condition 1)), it is necessary to specify a point belonging to the  $\text{int} G_\varphi(t_f)$ . As such a point (similarly to Section 7), take the point generated by the constant control  $u(t) \equiv \varphi/t_f$ . Thus, condition 1) of Lemma 5.3 is satisfied for  $M = M_\varphi(t_f)$ .

As a result, for all the variants (considered in Section 9.2) of Case 3, we obtain the fulfillment of Lemma 5.3 conditions. So,  $M_\varphi(t_f) = \text{int} \mathbf{A}_\varphi(t_f) \subset G_\varphi(t_f)$ . Hence, taking into account (9.3), we get  $G_\varphi(t_f) = \mathbf{A}_\varphi(t_f)$  in Case 3. As a consequence, for the degenerate subcase under  $\varphi < \pi$ , we have  $\mathcal{P}_{2,6} = \mathcal{P}_{3,6} \in \text{int} G_\varphi(t_f)$ .

The boundary of the set  $G_\varphi(t_f)$  is made up of the curve A1 and the part of the curve A3 to the first point of its intersection with the axis  $X$  as well as the symmetric part of the curve A2 (see Figs. 17 and 18). Fig. 18a (Fig. 18b) corresponds to  $t_f = 4.5\pi$ ,  $\varphi = \pi$  ( $t_f = 8.5\pi$ ,  $\varphi = \pi$ ).

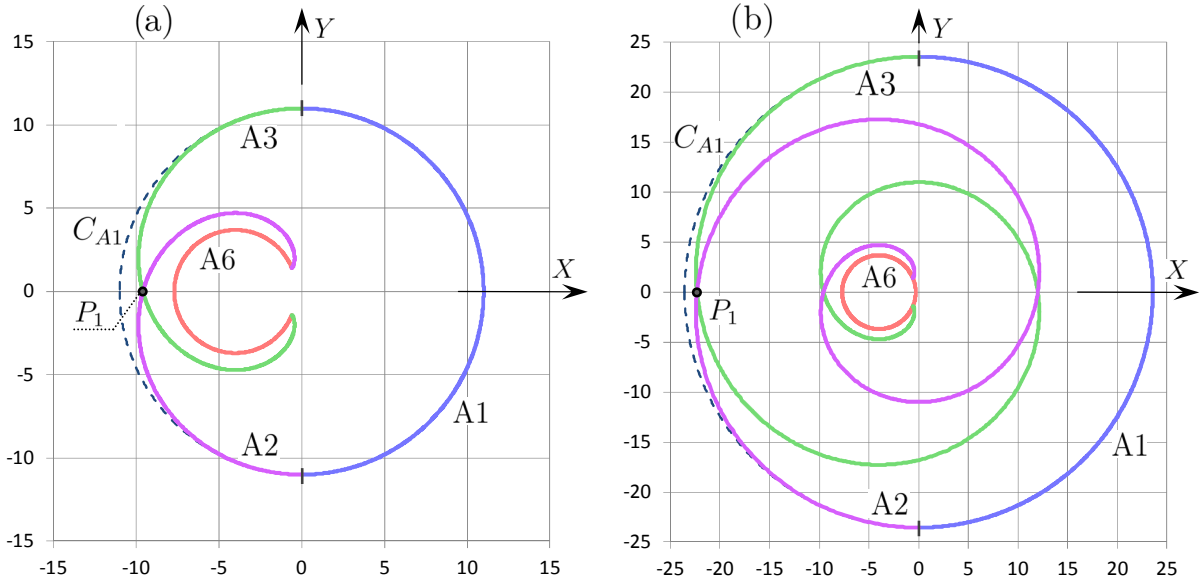
**Remark 9.1.** Consider the degenerate subcase (9.2) of Case 3.

Under the condition  $\varphi \geq \pi$  (Section 9.2, subpoint 2.2, Fig. 17b and 17c), the point  $H$  lies on the boundary of the set  $G_\varphi(t_f)$ . Therefore, the point  $(H, \varphi)^\top$  belongs to the boundary of the three-dimensional set  $G(t_f)$ .

Under the condition  $0 \leq \varphi < \pi$  (Section 9.2, subpoint 2.1, Fig. 17a), we have  $H \in \text{int} G_\varphi(t_f)$ . If  $0 < \varphi < \pi$ , then with a fixed value of  $t_f$ , the point  $H$  is the limit for the arc  $A6(\tilde{\varphi})$ , where  $0 < \tilde{\varphi} < \varphi$  and  $\tilde{\varphi} \rightarrow \varphi$ . Since for any point  $P \in A6(\tilde{\varphi})$ , the inclusion  $P \in \partial G_{\tilde{\varphi}}(t_f)$  is performed, then  $(P, \tilde{\varphi})^\top \in \partial G(t_f)$ . Hence, taking into account the closedness of the set  $G(t_f)$ , we obtain  $(H, \varphi)^\top \in \partial G(t_f)$ .

Thus, in the whole, for the degenerate subcase (9.2) of Case 3, the point  $(H, \varphi)^\top$  belongs to the boundary of the three-dimensional reachable set  $G(t_f)$  for  $\varphi > 0$ . If  $\varphi = 0$ , then the point  $(H, \varphi)^\top$  belongs to the interior of the three-dimensional reachable set  $G(t_f)$ .



FIGURE 18. Case 3. The set  $G_\varphi(t_f)$  in the non-degenerate subcase

#### 10. BOUNDARY OF $\varphi$ -SECTIONS FOR CASE 4

Let us show that in Case 4 any  $\varphi$ -section is the circle  $C_{A1}$  given by the curve A1. The position of the center of the circle depends on  $\varphi$ , and its radius depends on  $\varphi$  and  $t_f$ .

The curve A1 is defined by formula (3.10) and is an arc of the circle with the radius  $R_{A1} = (t_f - \varphi)$  and with the center at the origin of the auxiliary coordinate system  $X, Y$ . By the definition of Case 4 (see (6.4)), the inequality  $\varphi \geq 2\pi$  holds. The arc A1, the span of which is equal to  $\varphi$ , forms a circumference with an “overlap”. The curves A2, A3, and A6 belong to the circle  $C_{A1}$ . Moreover, the points  $\mathcal{P}_{1,2}$  and  $\mathcal{P}_{1,3}$  (where the curves A2 and A3 are joining with the curve A1) lie on its boundary. All other points of the curves A2 and A3, as well as all the curve A6, are located in the  $\text{int}C_{A1}$  (Section 3.7, Property 8).

Let us establish that all points of the curves A2, A3, and A6 lying in the  $\text{int}C_{A1}$  belong to the  $\text{int}G_\varphi(t_f)$ . The interior points of the curve A3 are generated by controls of the type U3 with three nondegenerate constancy intervals (Section 3.7, Property 4). Here, the switch instants  $t_1$  and  $t_2$  are defined by the relation  $\varphi = t_1 - (t_f - t_2)$ . Since  $\varphi \geq 2\pi$ , so,  $t_1 > t_1 - (t_f - t_2) \geq 2\pi$ . Therefore, on all motions leading to the inner points of the curve A3, there is a cycle on the first interval of control constancy. Thus, in accordance with Lemma 4.1, we obtain that the points of the curve A3 under consideration belong to  $\text{int}G_\varphi(t_f)$ . The similar property is valid for the curve A2.

Consider the curve A6. It is generated by controls of the type U6. The corresponding switch instants  $t_1$  and  $t_2$  are defined by the relations

$$t_f = (t_1 - t_0) + (t_2 - t_1) + (t_f - t_2), \quad \varphi = -(t_1 - t_0) + (t_2 - t_1) - (t_f - t_2).$$

From here,  $(t_2 - t_1) = (t_f + \varphi)/2$ . From condition (6.4), we get  $2\pi < (t_2 - t_1) < t_f$ . Thus, for any point of the curve A6 on the corresponding control, duration of the second interval is greater than  $2\pi$ , and at least one of the two adjacent extreme intervals is not degenerate. By Lemma 4.2, we conclude that the curve A6 entirely belongs to the  $\text{int}G_\varphi(t_f)$ .

Using Lemma 5.1 and Lemma 5.3, we obtain  $G_\varphi(t_f) = C_{A1}$ .

Figure 19a (19b) shows the set  $G_\varphi(t_f)$  for the values  $t_f = 5\pi$  and  $\varphi = 2.5\pi$  (correspondingly,  $t_f = 8\pi$  and  $\varphi = 2.5\pi$ ). It coincides with the circle  $C_{A1}$ . The curve A1 is the circumference with an “overlap”. The curves A2, A3, and A6 are also shown.

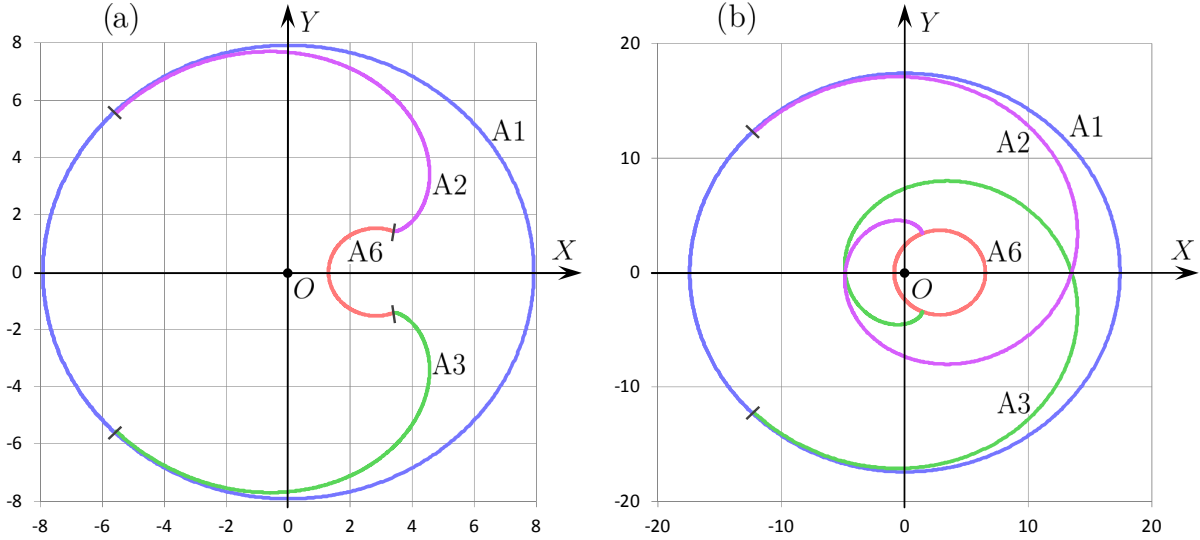


FIGURE 19. Case 4. The set  $G_\varphi(t_f)$  for two variants  $t_f$  and  $\varphi$

## 11. GENERAL DESCRIPTION OF THE STRUCTURE OF $\varphi$ -SECTIONS FOR $\varphi \geq 0$

We summarize the results of Sections 6 – 10 on the structure of the  $\varphi$ -sections of the reachable set for  $\varphi \geq 0$  in the following statement.

**Theorem 11.1.** *Let  $\varphi \geq 0$ . Then*

1) *the  $\varphi$ -sections  $G_\varphi(t_f)$  of the reachable set  $G(t_f)$  are simply connected in Cases 1, 3, 4, 5. In Case 2, the  $\varphi$ -section  $G_\varphi(t_f)$  is not simply connected;*

2) *in Case 1, the boundary of the  $\varphi$ -section  $G_\varphi(t_f)$  is a simple closed curve  $A_\varphi(t_f)$  composed of successively connected curves A1, A3, A6, and A2;*

3) *in Case 2, the boundary of the  $\varphi$ -section  $G_\varphi(t_f)$  splits into two parts: the outer contour (the curve  $A_\varphi(t_f)$ ) and the inner contour (the curve  $B_\varphi(t_f)$ ). The outer contour is made up of the curve A1 and adjacent parts of the curves A2 and A3 up to the point  $P_1$  of their first intersection. The inner contour is made up of the curve A6 and adjacent parts of the curves A2 and A3 up to the point  $P_2$  of their last intersection;*

4) *in Case 3, the boundary of the  $\varphi$ -section  $G_\varphi(t_f)$  is a simple closed curve  $A_\varphi(t_f)$ . It consists of the curve A1 and adjacent parts of the curves A2 and A3 up to the point  $P_1$  of their first intersection;*

5) *in Case 4, the boundary of the  $\varphi$ -section  $G_\varphi(t_f)$  is a circumference defined by the curve A1;*

6) *in Case 5, the  $\varphi$ -section  $G_\varphi(t_f)$  degenerates to a point.*

12. CASE  $\varphi < 0$ 

Study of the case  $\varphi < 0$  is based on the symmetry property of system (2.1), which is the following. Consider the motion  $(x^*(t), y^*(t), \varphi^*(t))^T$  of the system on the interval  $[0, t_f]$  from the initial zero phase point generated by some admissible control  $u^*(t)$ . At the instant  $t_f$ , we get the point  $(x^*(t_f), y^*(t_f), \varphi^*(t_f))^T$ . The control  $u_*(t) = -u^*(t)$  (i.e., it differs from the initial one only in sign) with the same zero initial phase point gives the phase state  $(x_*(t_f), y_*(t_f), \varphi_*(t_f))^T$  at the instant  $t_f$  where  $x_*(t_f) = x^*(t_f)$ ,  $y_*(t_f) = -y^*(t_f)$ ,  $\varphi_*(t_f) = -\varphi^*(t_f)$ .

This leads to the fact that the  $\varphi^*$ -section  $G_{\varphi^*}(t_f)$  of the reachable set  $G(t_f)$  for any  $\varphi^*$  is associated with the corresponding section for  $\varphi_* = -\varphi^*$  by mirroring about the axis  $x$  of the original coordinate system. Within the framework of the auxiliary coordinate system (if it is also introduced for  $\varphi < 0$ ), the new section coincides with the old one. Such facts make it possible not to consider separately the case  $\varphi < 0$ . The result for it is determined by the case  $\varphi > 0$ .

For  $\varphi = 0$ , the original coordinate system  $x, y$  coincides with the auxiliary system  $X, Y$ . Therefore, the corresponding  $\varphi$ -section  $G_\varphi(t_f)$  is symmetric w.r.t. the axis  $x$  of the original coordinate system.

**Remark 12.1.** The material of Sections 6–10 can be interpreted as a description of additional conditions imposed onto controls of the type U1 – U6 from (3.1). Such conditions (along with relation (3.2)) select controls leading to the boundary of the  $\varphi$ -sections of the reachable set  $G(t_f)$ . These conditions depend on  $t_f$  and  $\varphi$  (see formulas (6.1)–(6.5) and Fig. 11). Taking them into account completely characterizes not only the boundary of the  $\varphi$ -sections, but, also, the boundary of the entire three-dimensional reachable set  $G(t_f)$ .

## CONCLUSION

For the Dubins car with symmetric control constraint, the analytical description is obtained for the sections along the angular coordinate  $\varphi$  of the three-dimensional reachable set  $G(t_f)$ . Possible types of the two-dimensional  $\varphi$ -sections of the set  $G(t_f)$  with different collections of boundary arcs are classified. The case is highlighted when the  $\varphi$ -section is not simply connected.

A certain class of piecewise constant controls with at most two switches was described in [40]. It was shown that we can restrict ourselves to such controls when constructing the boundary of the three-dimensional reachable set. However, in this class, there were also controls leading to the interior of the reachable set. The relations obtained in this paper filter out such controls. Thus, a subclass of controls is singled out, each of which leads to the boundary of the reachable set. On the contrary, for each point of the boundary, there is at least one control from the given subclass leading to this point.

The paper results open up the possibility (based on the effective numerical construction of the set  $G(t_f)$  boundary with the growth of  $t_f$ ) to solve many problems of optimal control with the dynamics of the Dubins car including the time-optimal problems. It is also possible to use the results obtained for solving some game problems.

The paper results are planned to carry over onto the case of an asymmetric constraint on the control  $u \in [u_1, u_2]$  for  $u_1 < 0$ ,  $u_2 > 0$ .

## Acknowledgements

This paper is dedicated to the memory of Professor Rafail Fedorovich Gabasov who was a student of E.A. Barbashin and N.N. Krasovskii. Together with E.A. Barbashin and F.M. Kirillova, he did a lot for the development of the theory of optimal control in Belarus, where he achieved remarkable scientific results and created a world-famous mathematical school. The authors thank M.A. Patrakeevev for consultations related to applications of the Jordan and Schoenflies theorems. The authors express their gratitude to S.I. Kumkov for his help in translating the text into English. The authors are grateful to the reviewer for useful comments.

## REFERENCES

- [1] Dubins, L. E., “On Curves of Minimal Length with a Constraint on Average Curvature and with Prescribed Initial and Terminal Positions and Tangents,” *American J. Math.*, Vol. 79, No. 3, 1957, pp. 497–516, doi: 10.2307/2372560.
- [2] Sussmann, H. J. and Tang, W., “Shortest Paths for the Reeds-Shepp Car: a Worked Out Example of the Use of Geometric Techniques in Nonlinear Optimal Control,” Report sycon-91-10, Rutgers University, 1991.
- [3] Kaya, C. Y., “Markov-Dubins Path via Optimal Control Theory,” *Computational Optimization and Applications*, Vol. 68, No. 3, 2017, pp. 719–747, doi:10.1007/s10589-017-9923-8.
- [4] Markov, A. A., “A Few Examples of Solving Special Problems on the Largest and Smallest Values,” *The communications of the Kharkov mathematical society*, Vol. 1, No. 2, 1889, pp. 250–276. (in Russian).
- [5] Isaacs, R., “Games of Pursuit,” Tech. rep., RAND Corporation, Santa Monica, 1951.
- [6] Miele, A., *Flight Mechanics, Volume 1: Theory of Flight Paths*, Addison-Wesley Publishing Company, London, 1962.
- [7] Pecsvaradi, T., “Optimal Horizontal Guidance Law for Aircraft in the Terminal Area,” *IEEE Trans. on Automatic Control*, Vol. 17, No. 6, 1972, pp. 763–772.
- [8] Laumond, J.-P., ed., *Robot Motion Planning and Control*, Springer-Verlag, Berlin; Heidelberg, 1998, doi: 10.1007/BFb0036069.
- [9] Hernandez, J. D., Moll, M., Vidal, E., Carreras, M., and Kavraki, L. E., “Planning Feasible and Safe Paths Online for Autonomous Underwater Vehicles in Unknown Environments,” in “2016 IEEE/RSJ International Conference on Intelligent Robots and Systems (IROS),” , 2016, pp. 1313–1320, doi:10.1109/IROS.2016.7759217.
- [10] LaValle, S. M., *Planning Algorithms*, Cambridge University Press, 2006.
- [11] Giordano, P. R. and Vendittelli, M., “Shortest Paths to Obstacles for a Polygonal Dubins Car,” *IEEE Transactions on Robotics*, Vol. 25, No. 5, 2009, pp. 1184–1191, doi:10.1109/TRO.2008.2011421.
- [12] Manyam, S., Rathinam, S., Casbeer, D., and Garcia, E., “Shortest Paths of Bounded Curvature for the Dubins Interval Problem,” arXiv:1507.06980v2, 2015.
- [13] Manyam, S. G., Casbeer, D. W., Moll, A. L., and Fuchs, Z., “Shortest Dubins Path to a Circle,” in “AIAA SciTech 2019 Forum,” San Diego, California, 2019, pp. 1–7, doi:10.2514/6.2019-0919.
- [14] Chen, Z., “On Dubins Paths to a Circle,” *Automatica*, Vol. 117, doi:10.1016/j.automatica.2020.108996.
- [15] Zheng, Y., Chen, Z., Shao, X., and Zhao, W., “Time-Optimal Guidance for Intercepting Moving Targets with Impact-Angle Constraints,” *Chinese Journal of Aeronautics*, doi:https://doi.org/10.1016/j.cja.2021.08.002.
- [16] Koval, A. and Isler, V., “Turning a Corner with a Dubins Car,” in “2019 International Conference on Robotics and Automation (ICRA),” 2019, pp. 8570–8576, doi:10.1109/ICRA.2019.8794361.
- [17] Lee, J. H., Cheong, O., Kwon, W. C., Shin, S. Y., and Chwa, K. Y., “Approximation of Curvature-Constrained Shortest Paths through a Sequence of Points,” in Paterson, M. S., ed., “Algorithms - ESA 2000,” Springer, Berlin, Heidelberg, 2000, pp. 314–325, doi:10.1007/3-540-45253-2\_29.
- [18] Berdyshev, Y. I., “On the Problem of Sequential Traversal of a Set of Smooth Manifolds by a Nonlinear Controlled Object,” *Differential Equations*, Vol. 38, No. 11, 2002, pp. 1541–1552, doi:10.1023/A:1023676619449.
- [19] Chen, Z. and Shima, T., “Shortest Dubins Paths through Three Points,” *Automatica*, Vol. 105, 2019, pp. 368–375.

- [20] Berdyshev, Y. I., “Optimal Control in a Nonlinear Sequential Rendezvous Problem,” *Journal of Computer and Systems Sciences International*, Vol. 58, No. 1, 2019, pp. 95–104.
- [21] Chen, Z., Wang, K., and Lu, Y., “Elongation of Curvature-Bounded Path,” arXiv:2109.02125v1, 2021.
- [22] Mitchell, I. M., Bayen, A. M., and Tomlin, C. J., “A Time-Dependent Hamilton-Jacobi Formulation of Reachable Sets for Continuous Dynamic Games,” *IEEE Transactions on Automatic Control*, Vol. 50, No. 7, 2005, pp. 947–957, doi:10.1109/TAC.2005.851439.
- [23] Meyer, Y., Isaiah, P., and Shima, T., “On Dubins Paths to Intercept a Moving Target,” *Automatica*, Vol. 53, 2015, pp. 256–263, doi:10.1016/j.automatica.2014.12.039.
- [24] Buzikov, M. E. and Galyaev, A. A., “Time-Optimal Interception of a Moving Target by a Dubins Car,” *Automation and Remote Control*, Vol. 82, No. 5, 2021, pp. 745–758, doi:10.1134/S0005117921050015.
- [25] Isaacs, R., *Differential Games*, John Wiley and Sons, New York, 1965.
- [26] Merz, A. W., *The Homicidal Chauffeur – a Differential Game*, Ph.D. thesis, Stanford University, 1971.
- [27] Coates, S., Pachter, M., and Murphey, R., “Optimal Control of a Dubins Car with a Capture Set and the Homicidal Chauffeur Differential Game,” *IFAC-PapersOnLine*, Vol. 50, No. 1, 2017, pp. 5091–5096, doi:10.1016/j.ifacol.2017.08.775.
- [28] Cacace, S., Lai, A. C., and Loreti, P., “Modeling and Optimal Control of an Octopus Tentacle,” *SIAM J. Control Optim.*, Vol. 58, No. 1, 2020, pp. 59–84, doi:10.1137/19M1238939.
- [29] Bakolas, E. and Tsiotras, P., “Optimal Synthesis of the Asymmetric Sinistral/Dextral Markov-Dubins Problem,” *Journal of Optimization Theory and Applications*, Vol. 150, No. 2, 2011, pp. 233–250.
- [30] Berdyshev, Y. I., “Time-Optimal Control Synthesis for a Fourth-Order Nonlinear System,” *J. Appl. Math. Mech.*, Vol. 39, No. 6, 1975, pp. 948–956.
- [31] Owen, M., Beard, R. W., and McLain, T. W., “Implementing Dubins Airplane Paths on Fixed-Wing UAVs,” in “Handbook of Unmanned Aerial Vehicles,” Springer, pp. 1677–1701, 2015.
- [32] Rubies-Royo, V., Fridovich-Keil, D., Herbert, S., and Tomlin, C. J., “A Classification-based Approach for Approximate Reachability,” in “2019 International Conference on Robotics and Automation (ICRA),” , 2019, pp. 7697–7704, doi:10.1109/ICRA.2019.8793919.
- [33] Matveev, A. S., Magerkin, V. V., and Savkin, A. V., “A Method of Reactive Control for 3D Navigation of a Nonholonomic Robot in Tunnel-Like Environments,” *Automatica*, Vol. 114, 2020, p. 108831, doi:10.1016/j.automatica.2020.108831.
- [34] Sultan, M. M., Biediger, D., Li, B., and Becker, A. T., “The Reachable Set of a Drone: Exploring the Position Isochrones for a Quadcopter,” in “2021 IEEE International Conference on Robotics and Automation (ICRA),” 2021, pp. 7679–7685, doi:10.1109/ICRA48506.2021.9561715.
- [35] Botkin, N. D., Hoffmann, K.-H., and Turova, V. L., “Stable Numerical Schemes for Solving Hamilton–Jacobi–Bellman–Isaacs Equations,” *SIAM Journal on Scientific Computing*, Vol. 33, No. 2, 2011, pp. 992–1007, doi:10.1137/100801068.
- [36] Takei, R. and R.Tsai, “Optimal Trajectories of Curvature Constrained Motion in the Hamilton–Jacobi Formulation,” *Journal of Scientific Computing*, Vol. 54, 2013, pp. 622–644.
- [37] Munts, N. V., “Numerical Study of Different Variants of Dubins’ Car Model,” in “Proceedings of the 60th Israel Annual Conference on Aerospace Sciences,” Tel-Aviv & Haifa, Israel, 2020, pp. 1006–1022.
- [38] Zimovets, A. A., Matviichuk, A. R., Ushakov, A. V., and Ushakov, V. N., “Stability Property in the Convergence Game Problem in the Presence of Phase Constraints,” *J. Comput. Syst. Sci. Int.*, Vol. 60, No. 4, 2021, pp. 530–548, doi:10.1134/S1064230721040110.
- [39] Cockayne, E. J. and Hall, G. W. C., “Plane Motion of a Particle Subject to Curvature Constraints,” *SIAM Journal on Control and Optimization*, Vol. 13, No. 1, 1975, pp. 197–220.
- [40] Patsko, V. S., Pyatko, S. G., and Fedotov, A. A., “Three-Dimensional Reachability Set for a Nonlinear Control System,” *Journal of Computer and Systems Sciences International*, Vol. 42, No. 3, 2003, pp. 320–328.
- [41] Pontryagin, L. S., Boltyanskii, V. G., Gamkrelidze, R. V., and Mischenko, E. F., *The Mathematical Theory of Optimal Processes*, Interscience, New York, 1962.
- [42] Lee, E. B. and Markus, L., *Foundations of Optimal Control Theory*, Wiley and Sons, New York, 1967.
- [43] Patsko, V. S. and Fedotov, A. A., “Three-Dimensional Reachable Set at Instant for the Dubins Car: Properties of Extremal Motions,” in “Proceedings of the 60th Israel Annual Conference on Aerospace Sciences,” Tel-Aviv & Haifa, 2020, pp. 1033–1049.

- [44] Patsko, V. S. and Fedotov, A. A., “Analytic Description of a Reachable Set for the Dubins Car,” *Trudy Instituta Matematiki i Mekhaniki URO RAN*, Vol. 26, No. 1, 2020, pp. 182–197, doi:10.21538/0134-4889-2020-26-1-182-197. (in Russian).
- [45] Savelov, A., *Planar curves*, Fizmatlit, Moscow, 1960. (in Russian).
- [46] Spiegel, M., *Mathematical Handbook of Formulas and Tables*, Schaum’s outline series, McGraw-Hill Book Company, 1968.
- [47] Kurnosenko, A. I., “An Inversion Invariant of a Pair of Circles,” *Journal of Mathematical Sciences*, Vol. 110, No. 4, 2002, pp. 2848–2860, doi:10.1023/A:1015310614585.
- [48] Filippov, A. F., “An Elementary Proof of Jordan’s Theorem,” *Uspekhi Mat. Nauk*, Vol. 5, No. 5, 1950, pp. 173–176. (in Russian).
- [49] Cairns, S. S., “An Elementary Proof of the Jordan-Schoenflies Theorem,” *Proceedings of the American Mathematical Society*, Vol. 2, No. 6, 1951, pp. 860–867.
- [50] Filippov, A. F., “On Certain Questions in the Theory of Optimal Control,” *J. SIAM Control; Ser. A*, Vol. 1, No. 1, 1962, pp. 76–84, doi:10.1137/0301006.